frontiers | Frontiers in Marine Science

ORIGINAL RESEARCH
published: 04 July 2022
doi: 10.3389/fmars.2022.899877

Coralline Algae at the Paleocene/Eocene Thermal Maximum in the Southern Pyrenees (N Spain)

Julio Aguirre[1*†], *Juan I. Baceta*[2†] *and Juan C. Braga*[1†]

[1] Dpto. Estratigrafía y Paleontología, Facultad de Ciencias, Universidad de Granada, Granada, Spain, [2] Departamento de Geología, Facultad de Ciencia y Tecnología, Universidad del País Vasco, Bilbao, Spain

During the Paleocene/Eocene Thermal Maximum, ~55.6 Ma, the Earth experienced the warmest event of the last 66 Ma due to a massive release of CO_2. This event lasted for ~100 thousands of years with the consequent ocean acidification (estimated pH = 7.8-7.6). In this paper, we analyze the effects of this global environmental shift on coralline algal assemblages in the Campo and Serraduy sections, in the south-central Pyrenees (Huesca, N Spain), where the PETM is recorded within coastal-to-shallow marine carbonate and siliciclastic deposits. In both sections, coralline algae occur mostly as fragments, although rhodoliths and crusts coating other organisms are also frequent. Rhodoliths occur either dispersed or locally forming dense concentrations (rhodolith beds). *Distichoplax biserialis* and geniculate forms (mostly *Jania nummulitica*) of the order Corallinales dominated the algal assemblages followed by Sporolithales and Hapalidiales. Other representatives of Corallinales, namely *Spongites*, *Lithoporella* as well as *Neogoniolithon*, *Karpathia*, and *Hydrolithon*, are less abundant. Species composition does not change throughout the Paleocene/Eocene boundary but the relative abundance of coralline algae as components of the carbonate sediments underwent a reduction. They were abundant during the late Thanetian but became rare during the early Ypresian. This abundance decrease is due to a drastic change in the local paleoenvironmental conditions immediately after the boundary. A hardground at the top of the Thanetian carbonates was followed by continental sedimentation. After that, marine sedimentation resumed in shallow, very restricted lagoon and peritidal settings, where muddy carbonates rich in benthic foraminifera, e.g., milioliids (with abundant *Alveolina*) and soritids, and eventually stromatolites were deposited. These initial restricted conditions were unfavorable for coralline algae. Adverse conditions continued to the end of the study sections although coralline algae reappeared and were locally frequent in some beds, where they occurred associated with corals. In Serraduy, the marine reflooding was also accompanied by significant terrigenous supply, precluding algal development. Therefore, the observed changes in coralline algal assemblages during the PETM in the Pyrenees were most likely related to local paleoenvironmental shifts rather than to global oceanic or atmospheric alterations.

Keywords: rhodolith beds, thermal maximum, paleocene/eocene boundary, ocean acidification, pyrenean basin

OPEN ACCESS

Edited by:
Gang Li,
South China Sea Institute of Oceanology, Chinese Academy of Sciences, China

Reviewed by:
Amit K. Ghosh,
Birbal Sahni Institute of Palaeosciences (BSIP), India
Sherif Farouk,
Egyptian Petroleum Research Institute, Egypt

***Correspondence:**
Julio Aguirre
jaguirre@ugr.es

†These authors have contributed equally to this work

Specialty section:
This article was submitted to Marine Ecosystem Ecology, a section of the journal Frontiers in Marine Science

Received: *19 March 2022*
Accepted: *23 May 2022*
Published: *04 July 2022*

Citation:
Aguirre J, Baceta JI and Braga JC (2022) Coralline Algae at the Paleocene/Eocene Thermal Maximum in the Southern Pyrenees (N Spain). Front. Mar. Sci. 9:899877. doi: 10.3389/fmars.2022.899877

INTRODUCTION

Recent studies on the present-day global change, particularly increasing temperature and ocean acidification linked to the massive release of greenhouse gasses to the atmosphere due to anthropogenic activities, are progressively demanding detailed analyses of events of similar magnitude throughout the Earth history (Ridgwell and Schmidt, 2010; Gattuso and Hansson, 2011; Hönisch et al., 2012; Hansen et al., 2013; Lunt et al., 2013; Zeebe and Zachos, 2013; Burke et al., 2018; Haynes and Hönisch, 2020). One of the targets is to analyze the effects of these global processes on marine calcified biota in the geological record to model and compare with the predicted biological changes for the future. The Paleocene/Eocene thermal maximum (PETM) is a spike-like thermal event (Kennett and Stott, 1991; Thomas and Shackleton, 1996), at which researchers are looking as an ancient analogue to understand the ongoing biotic changes (Zeebe and Westbroek, 2003; Sluijs et al., 2007; Ridgwell and Schmidt, 2010; McInerney and Wing, 2011; Zeebe and Ridgwell, 2011; Hönisch et al., 2012; Zeebe, 2012; Norris et al., 2013; Zeebe and Zachos, 2013; Mudelsee et al., 2014; Haynes and Hönisch, 2020).

During the Paleocene/Eocene boundary ~55.6 million years ago (Ma), the Earth witnessed the warmest event of the last 66 Ma due to a huge delivery of CO_2 to the atmosphere mostly linked to volcanism (Haynes and Hönisch, 2020). This event is recorded by an abrupt negative carbon stable isotope ($\delta^{13}C$) excursion (CIE) (Koch et al., 1992). It is estimated that about 1,500 ppmv of CO_2 were released to the atmosphere during a short time interval of 120-220 thousands of years (kyr) (e.g., Sluijs et al., 2007; McInerney and Wing, 2011) or even less (Kennett and Stott, 1991; Zachos et al., 2005). The most recent time model suggests that there was a first pulse of CO_2 release 5-6 kyr after the CIE that was followed by sustained high values for ca. 40 kyr and ended ~100 kyr (Haynes and Hönisch, 2020). As a consequence, ocean pH decreased to 7.8-7.6 and global ocean surface temperature increased 5-9°C (Zachos et al., 2005; Zachos et al., 2008; McInerney and Wing, 2011; Zeebe and Ridgwell, 2011; Zeebe, 2012; Norris et al., 2013; Zeebe and Zachos, 2013; Mudelsee et al., 2014; Haynes and Hönisch, 2020).

Despite the drastic atmospheric, temperature, and oceanic alterations taking place during the PETM, only deep-sea benthic foraminifera were significantly affected, and 35-50% of the species became extinct (Thomas, 1990; Thomas, 2007; Alegret et al., 2009a; Alegret et al., 2009b), whereas the event had a lesser impact on marginal platform inhabitants (Thomas, 2003; Alegret et al., 2005). Coral reef ecosystems also showed considerable reduction in coral species diversity, number of reef sites, reef size, and reef carbonate production during the Paleocene/Eocene boundary (Flügel and Kiessling, 2002; Schneibner and Speijer, 2008; Kiessling, 2010; Perrin and Kiessling, 2010). Norris et al. (2013) called this reef collapse as the early Eocene reef gap.

Larger benthic and planktonic foraminifera, calcareous nannoplankton and deep-sea ostracods experienced diversity turnovers during the PETM (Schaub, 1951; Hottinger, 1960; Canudo and Molina, 1992; Canudo et al., 1995; Kelly et al., 1998; Speijer and Morsi, 2002; Scheibner et al., 2005; Gibbs et al., 2006a; Gibbs et al., 2006b; Speijer et al., 2012). In addition, aberrant forms (teratologies) of calcareous nannoplankton (Raffi and De Bernardi, 2008), as well as dwarfism in deep-sea ostracods (Yamaguchi et al., 2012), have been recorded.

Coralline algae, fully calcified marine autotrophic organisms, are one of the most endangered algal groups due to global temperature increase and ocean acidification (e.g., Martin and Hall-Spencer, 2017; Cornwall et al., 2021). Laboratory studies and field observations indicate that coralline algae might be negatively affected due to ocean acidification derived from the greenhouse gasses release (Anthony et al., 2008; Hall-Spencer et al., 2008; Martin and Gattuso, 2009; Büdenbender et al., 2011; Diaz-Pulido et al., 2012; Kamenos et al., 2013; Guy-Haim et al., 2016; Martin and Hall-Spencer, 2017; Peña et al., 2020a; Cornwall et al., 2021). Nonetheless, contradictory or non-conclusive results have also been obtained (Martin and Hall-Spencer, 2017; Peña et al., 2020a; Cornwall et al., 2021; and references therein) due to acclimation of coralline algae to acidification, physiological advantages (pre-adaptations) or interaction with other non-calcified epiphytes growing on corallines (Martin and Hall-Spencer, 2017; Guy-Haim et al., 2020; Peña et al., 2020a; Cornwall et al., 2021).

In order to explore the long-term effects of the global change on coralline algae and their biological/evolutionary responses to these environmental alterations, here we analyzed coralline algal assemblages across the Paleocene/Eocene boundary and the PETM. The main aim was to assess how behaved/responded coralline algae to this major temperature change and ocean acidification event. We studied the classical sections of Campo and Serraduy, in the south-central Pyrenees (Huesca province, N Spain), which record upper Thanetian and lower Ypresian shallow-water carbonates as well as the PETM. These sections have been largely studied mostly focusing on the stratigraphy, sedimentology, biostratigraphy, and geochemistry across the Paleocene/Eocene interval (Eichenseer and Luterbacher, 1992; Payros et al., 2000; Pujalte et al., 2000a; Pujalte et al., 2000b; Orue-Etxebarria et al., 2001; Molina et al., 2003; Pujalte et al., 2003; Schmitz and Pujalte, 2003; Schmitz and Pujalte, 2007; Scheibner et al., 2007; Domingo et al., 2009; Pujalte et al., 2009a; Pujalte et al., 2009b; Robador et al., 2009; Arostegi et al., 2011; Baceta et al., 2011; Manners et al., 2013; Pujalte et al., 2014; Hamon et al., 2016; Duller et al., 2019; Li et al., 2020; Serra-Kiel et al., 2020; Pujalte et al., 2022). Regarding the fossil content, studies have focused mostly on planktonic and benthic foraminifera (both larger and small forms) as well as corals (Serra-Kiel et al., 1994; Orue-Etxebarria et al., 2001; Molina et al., 2003; Scheibner et al., 2007; Li et al., 2020; Serra-Kiel et al., 2020). Nonetheless, no detailed analysis of the coralline algae throughout the Paleocene-Eocene transition has been carried out. We analyze the type of occurrence, species diversity and relative abundance of coralline algae with respect to other fossils throughout the late Thanetian (late Paleocene)-early Ypresian (early Eocene) interval to check how global alterations during the PETM affected coralline algae. In the case of rhodoliths, we also examine the coralline algal growth forms, as well as the inner algal arrangements and external morphology.

GEOLOGICAL SETTING

The Pyrenees is a reference area in Western Europe for the study of Paleogene shallow to deep-marine deposits and the series of distinct biotic and physical events that punctuated the beginning of the Cenozoic. During the Paleocene and early Eocene, the Pyrenean basin was a large marine embayment opening to the Bay of Biscay, to the WNW, with a central (hemi)pelagic trough flanked on the north, south and east by extensive shallow marine carbonate platforms (Baceta et al., 2004; Baceta et al., 2011) (**Figure 1A**). The platform systems evolved with general ramp profiles and most sectors exhibit a wide range of carbonate facies representative of beaches, tidal flats, lagoons, seagrass banks, shoals, tidal bars and a variety of reefal constructions. Most inner to mid ramp lithofacies are relatively rich in photic-dependent organisms (calcareous red algae, corals, larger benthic foraminifera –LBF–) and also comprise a varied heterozoan biota, represented by mollusks, bryozoans, echinoderms (Eichenseer, 1988; Serra-Kiel et al., 1994; Baceta, 1996; Baceta et al., 2004; Robador, 2008; Baceta et al., 2011). Landwards, the platform successions interfinger with siliciclastic and mixed sediments with subordinate evaporites and discontinuous paleosols, known as the Garumnian facies, which represent alluvial to coastal plain depositional environments (**Figure 1A**).

Sedimentation during the Paleocene and early Eocene in the Pyrenean basin margins evolved under general transgressive conditions, punctuated by a number of third order relative sea-level falls of variable magnitude and regional extent. These sea level drops are recorded by abrupt facies shifts and more or less prominent erosional discontinuities, commonly associated to enhanced subaerial exposure. Based on mapping and regional correlation, up to five depositional sequences recording shallow marine settings have been distinguished within the upper Thanetian-lower Ypresian succession (Eichenseer and Luterbacher, 1992; Baceta, 1996; Baceta et al., 2004; Baceta et al., 2011).

Our study focuses on the Paleocene to lower Eocene coralline red algae recorded in the Campo and Serraduy sections, which form part of continuous outcrops along the Ferrera and Morillo-Merli ridges, on the northern flank of the Tremp-Ainsa area (**Figure 1B**). Previous studies in these two sections and on coeval outcrops in the whole Tremp-Ainsa area have provided a well-constrained stratigraphic framework for the alluvial-coastal to

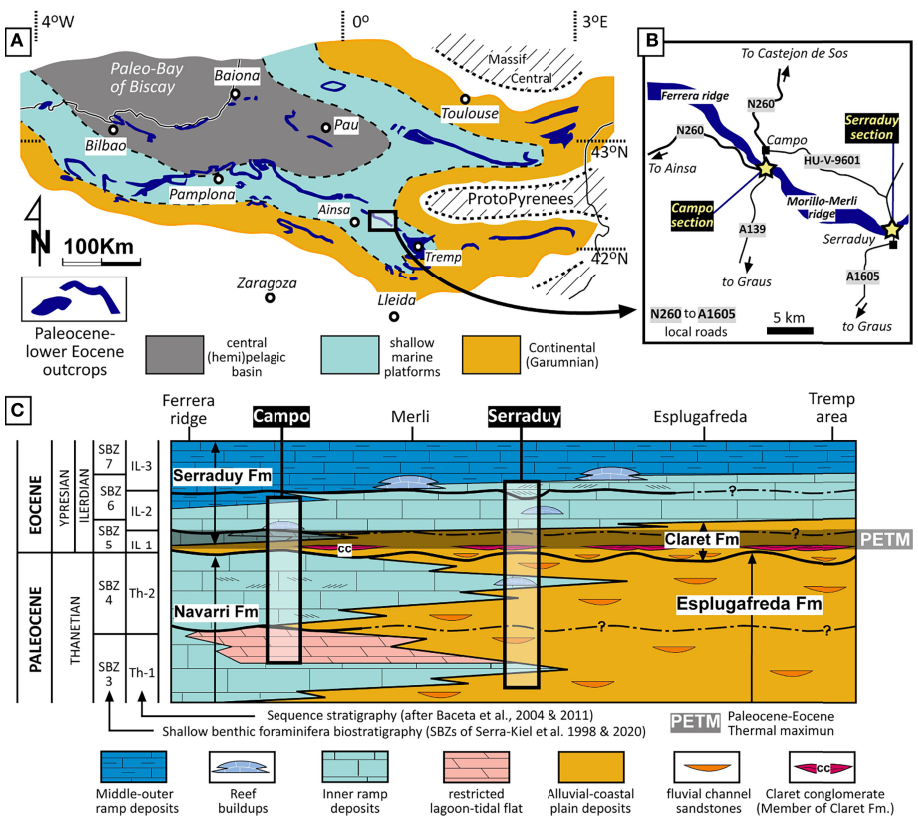

FIGURE 1 | **(A)** General paleogeography of the Pyrenean area during the earliest Eocene, at the time of the so-called Ilerdian transgression (adapted from Baceta et al., 2004). **(B)** Enlarged geographic map of part of the Ainsa-Tremp sector of the Pyrenean basin with location of the Campo and Serraduy sections (yellow starts). **(C)** Integrated stratigraphy of the upper Paleocene-lowermost Eocene strata of the Ainsa-Tremp area (adapted from Baceta et al., 2011; Pujalte et al., 2014). The rectangles indicate the position of the two study stratigraphic sections within the general stratigraphic framework.

shallow marine successions embedding the PETM event (e.g., Eichenseer, 1988; Payros et al., 2000; Baceta et al., 2004; Baceta et al., 2011). A detailed biostratigraphic scheme has been proposed based on LBF biozonation calibrated with standard calcareous plankton zonations and magnetostratigraphy (e.g., Hottinger and Schaub, 1960; Schaub, 1973; Serra-Kiel et al., 1994; Serra-Kiel et al., 1998; Orue-Etxebarria et al., 2001; Pujalte et al., 2009b; Serra-Kiel et al., 2020) (**Figure 1C**).

The upper Paleocene to lower Eocene strata of the area involves the interbedding of four lithostratigraphic formations (**Figure 1C**). The Esplugafreda and Claret Formations are made up of siliciclastic deposits formed in alluvial to coastal settings. The Navarri and Serraduy Formations are dominated by carbonate lithofacies representing coastal, lagoonal and shallow marine environments. In terms of sequence stratigraphy, the upper Paleocene Esplugafreda and Navarri Formations embrace two third-order depositional sequences (the Th-1 and Th-2) and the lower Ypresian Claret and Serraduy Formations comprise three depositional sequences (IL-1, IL-2 and IL-3) (**Figure 1C**). The PETM, as determined from detailed geochemical and isotopic studies (Pujalte et al., 2014; Pujalte et al., 2022) lies within the lowermost Ypresian IL-1 sequence, encompassing most of the alluvial Claret Fm. and the lowermost marine deposits of the Serraduy Formation (**Figure 1C**).

According to paleogeographic reconstructions of the area (Pujalte et al., 2014), the Serraduy section represents a shallower position relative to the Campo section. This is clearly evidenced by the architecture of the upper Paleocene succession, which at Campo section mainly consists of shallow marine carbonates, whereas at Serraduy section it is mostly made up of continental Garumnian facies. In both sections, the early Eocene comprises coastal and shallow-marine carbonates defining a deepening succession that culminates with middle to outer ramp deposits. In most outcrops of the Tremp-Ainsa area, the PETM event lies within continental siliciclastic deposits. In the Campo section, it is recorded within an interval of continental clastics with discontinuous palustrine carbonates passing vertically to inner ramp and restricted tidal flat carbonates (**Figure 1C**). The vertical facies succession of the Paleocene-lower Eocene deposits exposed at Campo and Serraduy is synthetized in **Figure 2**.

STRATIGRAPHIC SECTIONS

Campo Section

This section is located along the banks of the Esera River, 1 km south from the village of Campo (**Figure 1B**). Three main outcrops (along the old road to Ainsa, the local road to Navarri, and the road from Campo to Graus) allow the bed-by-bed analysis of 173 m of the upper Paleocene to lower Eocene deposits (**Figure 2A**). Sampling was focused in two intervals. The lower one comprises the uppermost 38 m of the Thanetian Th-2 sequence, which is made up of middle ramp bioclastic carbonates

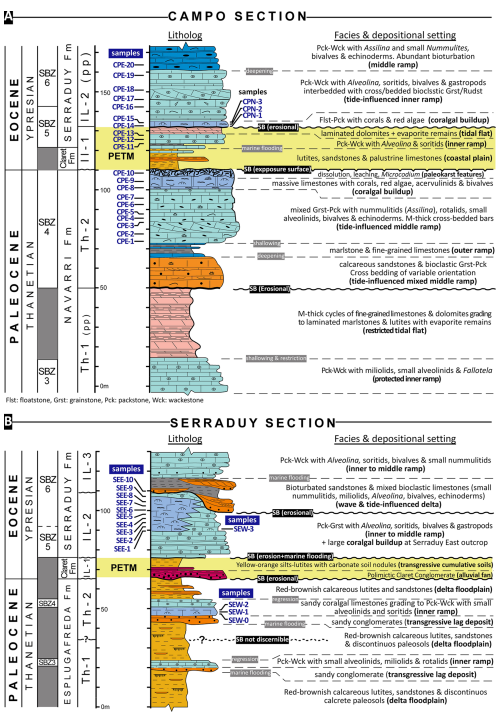

FIGURE 2 | Stratigraphic logs of the Campo **(A)** and Serraduy **(B)** sections, with indication of facies, main intervals, stratigraphic sequences (Th and IL), biostratigraphy, and the location of the samples studied for coralline algae (after Eichenseer, 1988; Serra-Kiel et al., 1994; Robador, 2008; Baceta et al., 2011; Serra-Kiel et al., 2020). Wck, Wackestone; Pck, Packstone; Grst, Grainstone; Rudst, Rudstone; Flst, Floastone; SB, Sequence boundary.

with decimeter- to meter-thick sigmoidal cross bedded tidal bars trending towards the east and southeast. This interval culminates with a massive muddy limestone rich in corals, red algae and mollusks, just below the prominent discontinuity at the top of the Th-2 sequence that marks the Paleocene-Eocene boundary. According to Serra-Kiel et al. (1994; 2020), the LBF assemblage of this upper part of the Th-2 sequence comprises *Glomalveolina levis*, *Assilina yvettae*, *A. azilensis*, and *Daviesina garumnensis*, all characteristic of the SBZ4 biozone of Serra-Kiel et al. (1998) (**Figure 2A**).

The upper interval, up to 41 m thick, belongs to the lower Eocene and comprises the upper part of the IL-1 and most of the IL-2 depositional sequences (**Figure 2A**). This interval mainly consists of shallow, inner-ramp carbonates rich in alveolinids, small milioliids, and soritids, associated with subordinate gastropods and bivalves (oysters and lucinids). A 2.5 m thick massive coral-rich limestone bed defining the base of sequence IL-2 was the only providing significant amounts of coralline algae. Therefore, this bed was sampled in two different outcrops: 1) samples CPE-14 and 15 on the new road to Graus, and, 2) samples CPN-1 to 3 on the old road to Ainsa. According to Serra-Kiel et al. (1994; 2020), this interval encompasses LBF association characteristic of the SBZ5 (*Alveolina vredenburgi*, *A. aramea*, *A. varians*) and the lower part of SBZ6 (*A. ellipsoidalis*, *A. pasticillata*, *A.* aff. *aragonensis*) (**Figure 2A**).

Serraduy Section

The Serraduy section is located 0.5 km north of Serraduy del Pont, on the Isabena valley, ~12 km to the SE of Campo (**Figure 1B**). Correlation through mapping of the outcrops on both river banks, the Serraduy East and Serraduy West, allowed analyzing in detail a 130 m thick section of upper Paleocene (66 m) and lower Eocene (64 m) deposits (**Figure 2B**).

The upper Paleocene is mostly siliciclastic and consists of red to brownish calcareous lutites with intercalations of medium to coarse-grained lithic sandstones forming lenses, sheets and discrete channel fills (alluvial floodplain deposits), and discontinuous development of calcrete paleosols. Two discrete intervals of shallow marine carbonates, respectively up to 4 and 8 m thick, define the maximum flooding stages within the upper Paleocene depositional sequences Th-1 and Th-2 (**Figures 1C**, **2B**). We sampled the upper one (Th-2 sequence) (**Figure 2B**). The lower beds of this upper limestone unit are sandy coralgal limestones, which are the only ones in the Thanetian of Serraduy section containing significant amount of red algae (samples SEW-0 to 2). According to Serra-Kiel et al. (1994; 2020), the lower limestone interval (Th-1 sequence) comprises a LBF assemblage of *Glomalveolina primaeva*, *Idalina sinjarica*, and *Miscellanea yvettae*, indicative of the SBZ3, whereas the upper limestone interval (Th-2 sequence) includes *Glomalveolina levis* and *Daviesina garumnensis*, two characteristic taxa of the SBZ4 (**Figure 2B**).

The lower Eocene deposits belong to depositional sequences IL-1 to IL-3 (**Figure 2B**). The IL-1 is entirely made up of continental deposits, including the characteristic Claret conglomerate member of the Claret Formation, which according to Pujalte et al. (2014; 2022) marks the beginning of the PETM event in the whole Tremp-Ainsa area.

The IL-2 consists of shallow marine carbonates. The bulk deposits correspond to bedded packstone-grainstones rich in alveolinids and soritids with a LBF assemblage of *Alveolina vredenbrigi*, *A. aramea* and *Opertorbitolites gracilis* (SBZ5) in the lower beds, and *A. ellipsoidalis*, *A. dolioliformis* and *Opertorbitolites* (lower part of SBZ6) in the upper beds (**Figure 2B**). On the Serraduy West outcrop, a bed with scattered corals 13 m above the base of the sequence is the only one with significant red algal content (samples SEW-3). On the east outcrops of the valley, a distinct massive bed package of coralgal limestones, up to 17 m thick, interfingers with the dominant *Alveolina*-rich deposits and comprises the main interval sampled for red algae (samples SEE-1 to 10) (**Figure 2B**). Eichenseer and Luterbacher (1992) interpreted these massive limestones as a low-relief coral biostrome.

The overlying IL-3 sequence rests unconformably onto the IL-2 sequence and consists mainly of bioturbated sandstones, silty marls, and sandy limestones that eventually form meter-thick tidal bars with sigmoidal cross bedding trending towards the northeast and southeast. The fossil content in the mixed deposits is a mixture of small nummulitids, milioliids, rare *Alveolina*, green algae (dasyclads), bivalves, echinoids and gastropods. Vertically, the basal mixed deposits of the IL-3 pass gradually into *Alveolina*-rich packstone-grainstones, similar to those defining the bulk of sequence IL-2. The LBF assemblage of these uppermost limestones comprises *Alveolina ellipsoidalis*, *A. dolioliformis*, *Glomalveolina lepidula*, *Opertorbitolites*, and *Nummulites bigurdensis*, defining the upper part of the SBZ6 (Serra-Kiel et al., 1998).

METHODS

Coralline algae occur mostly as fragments, which do not preserve enough taxonomic features to be identified at any precise taxonomic level. In these cases, we estimate the relative abundance of coralline algal fragments using the charts of Baccelle and Bosellini (1956).

In the upper Thanetian carbonates, coralline algae occur forming rhodoliths concentrated in particular beds. Here, preservation of the coralline algae is better allowing more precise taxonomic identifications. In these cases, the relative abundance of species was quantified by point-counting the area occupied by each taxon (Perrin et al., 1995). We identified the coralline algae at the lowest possible taxonomic level, in most cases at species level. When the specimens could not be confidently assigned to a described species, we used an open specific nomenclature. The taxonomic schemes of orders, families, subfamilies and genera follow recent molecular phylogenies (Peña et al., 2020b; Jeong et al., 2021).

The external rhodolith morphology was examined in different 2-D sections at the outcrops, as extraction of complete and isolated rhodoliths was impossible due to cementation of limestones. The internal arrangement, algal growth form, and

algal composition of rhodoliths were analyzed in thin sections. We use the terminology proposed by Woelkerling et al. (1993), as well as the recent terminology updated by Aguirre et al. (2017).

All data are compiled in **Table 1**, and a discussion of some of the identified taxa is provided in the Taxonomic Appendix.

RESULTS

Coralline Algal Occurrences

Most of the coralline algae occur as fragments in rudstone, grainstone and packstone lithofacies. They occur with other bioclasts, mostly, larger and small benthic foraminifers, corals, mollusks, bryozoans, echinoids, serpulids, and barnacles, as well as additional rhodophytes, such as *Marinella lugeoni* Pfender 1939 and the peyssonneliacean *Polystrata alba*, (Pfender) Denizot 1968 and chlorophytes of the orders Dasycladales and Bryopsidales (*Halimeda* spp) (**Figure 3**).

Coralline algal fragments are small (up to 2 mm; very exceptionally larger) and abraded due to reworking (**Figures 4A, B**). In both sections, coralline algae represent up to 30% of the rock volume in the upper Thanetian sediments. The proportion decreases substantially in the lower Ypresian deposits, with values ranging from 1 to 5% (exceptionally, up to 10% in sample CPE-15).

Due to high fragmentation and abrasion in these lithofacies, most coralline algal remains do not show diagnostic characteristics to be properly identified, even at family and order levels. Nonetheless, in some fragments reproductive structures are preserved allowing their identification. In the case of *Distichoplax biserialis*, the characteristic laminar growth forms and the isobilateral cell arrangements facilitate its identification.

In the small coral buildups found both in the upper Thanetian and lower Ypresian deposits, coralline algae occur as fragments in the matrix and as thin laminar crusts attached to corals (**Figures 4C, D**). More rarely, they form small rhodoliths with bioclastic nuclei, mostly corals or other algal fragments (**Figure 4E**).

Coralline algae also occur loosely to densely packed in rhodolith beds (Aguirre et al., 2017), such as those found in the upper part of the Navarri Formation in the Campo section (samples CPE-8 and CPE-10) (**Figures 5A–E**). The loosely packed beds consist of ellipsoidal rhodoliths, from 1 to 3 cm in largest diameter, made up of encrusting to warty corallines (**Figures 5A, C**). They are embedded in a fine-grained packstone-wackestone matrix with accompanying organisms such as echinoids, benthic foraminifers, and bryozoans. Densely packed rhodolith beds contain spheroidal to ellipsoidal rhodoliths, up to 7 cm in largest diameter, consisting of encrusting, fruticose and warty corallines (**Figures 5B, D, E**). In this case, rhodoliths are included in a packstone (rarely grainstone) matrix.

Internally, rhodoliths are either multispecific or monospecific (**Figure 6**). They are built up by coralline algae intergrown with encrusting foraminifera (mainly *Solenomeris*), serpulids, bryozoans, and *Polystrata alba* (**Figures 3A**, **6**). The nuclei of rhodoliths consist of lithoclasts or bioclasts, such as corals (**Figures 5F**, **6**). Internal voids are filled with the matrix sediment or are open and later filled up with cement. In some cases, rhodoliths are asymmetrical and geopetal structures indicate that the preferential algal growth coincided with the upright position of the rhodolith. This suggests that rhodoliths are preserved in their original growth position, without substantial reworking.

Coralline Algal Diversity

The orders Corallinales, Hapalidiales, and Sporolithales are represented throughout the late Thanetian-early Ypresian interval in the study sections, being the two former groups the most diversified (**Table 1**; **Figure 7**). In the late Thanetian, coralline assemblages include up to 16 species. Maximum coralline diversification is found in the coral floatstone facies sampled at Serraduy section (samples SEW-0 and SEW-1) (**Figures 2B**, **7**). The three algal orders underwent a drastic reduction in the number of species in the earliest Ypresian, with a virtual disappearance within the first marine beds encompassing and immediately above the PETM at the Campo section. Here, the limestones were almost exclusively dominated by LBF packstones-grainstones, with alveolinids and subordinate soritids. After this interval, the species richness of corallines increases in the early Ypresian. This diversity recovery is associated with the development of coral buildups at the base of IL-2 in both Campo and Serraduy sections.

The estimation of the relative abundance of species is hampered by preservation. Among the easily identifiable ones, the best represented is *Distichoplax biserialis*, which occurs in all samples, followed by geniculate species. The abundance of *D. biserialis* embedded in a packstone-wackestone matrix found in the uppermost Thanetian carbonates in the Campo section (samples CPE-9 and CPE-10) is remarkable, as it ranges from 73% to 95% of the coralline assemblages (**Figure 8**).

In contrast, preservation of coralline algae in the upper Thanetian rhodolith beds of Campo allows estimating species abundance. Here, members of the order Sporolithales were the most abundant (up to 75%), being *Sporolithon lugeoni* the best-represented species, followed by *Spongites* sp. 1, a few Hapalidiales, and anecdotal presence of laminar crusts of *Lithoporella* spp.

The thin laminar algae encrusting corals, both in the Thanetian and in the Ypresian, are mostly *Lithoporella* spp, and *Lithothamnion crispithallus* and *Lithothamnion* sp 5.

DISCUSSION

Paleoenvironmental Evolution

High fragmentation and rounding of coralline algae and other bioclasts, in the cross-bedded deposits defining the lower part of the upper Thanetian Navarri Formation indicate high-energy conditions in an open inner ramp setting. Dominance of Corallinales is consistent with these shallow water conditions (Braga and Martín, 1988; Braga and Aguirre, 2001; Braga and

TABLE 1 | Coralline algal species distribution in the two study sections, indicating presence (X) of each taxon in the samples.

							HAPALIDIALES											SPOROLITHALES					CORALLINALES																				OTHER		
Age	**Sample**	**N° of thin sections**	**Microfacies**	**CCA in matrix**	**Rhodoliths**		***Lithothamnion concretum* Howe**	***L. camarasae* Pfender**	***L. cf. corallinaeforme* Lemoine**	***L. cf. exuberans* Mastrorilli**	***L. crispithallus* Johnson**	***L. vaughani* Howe**	***Lithothamnion* sp.1**	***Lithothamnion* sp. 2**	***Lithothamnion* sp. 3**	***Lithothamnion* sp. 4**	***Lithothamnion* sp. 5**	**Undifferentiated Hapalidiales**	***Melobesia* sp.**	***Sporolithon lugeonii* Pfender**	***S. cf. oulianovii* Pfender**	***S. brevium*/*airoldii***	***Sporolithon* sp. 1**	**Undifferentiated Sporolithales**	***Jania nummulitica* Lemoine**	**Geniculate sp. 1 cf. *Corallina prisca* Johnson**	**Geniculate sp. 2**	**Geniculate sp. 3**	**Undifferentiated geniculates**	***Lithoporella minus* Johnson**	***Lithoporellamelobesioides* (Foslie) Foslie**	***Distichoplax biserialis* Dietrich**	***Spongites* sp. 1**	***Spongites* sp.2**	***Spongites* sp. 3**	***Hydrolithon lemoinei* (Miranda) Aguirre et al.**	***Karpathia sphaerocellulosa* Maslov**	**Undifferentiated Corallinales**	***Polystrata alba* (Pfender) Denizot**	***Marinella lugeonii* Pfender**	**Dasycladales**	**Halimedales**
	Campo section																																											
early Ypresian	CPE-20	1	Wck.-Pck. Miliolids+Nummulitids	0%																																								
	CPE-19	1	Pck.-Grn. Alveolina+Miliolids	0%																																								
	CPE-18	1	Grn. Alveolina+Miliolids	0%																																								
	CPE-17	1	Sandstone Miliolids+Alveolina	0%																																								
	CPE-16	1	Pck-Grn. Alveolinas	0%																																								
	CPE-15	4	Flst.(Frm.) Corals+CCA crusts+Miliolids	5-10% Dispersed rhodos.	CPN-3					x	x	x			x			x					x		x					x	x	x						x		x	x
	CPE-14	1	Pck.-Wck. Miliolids+oysters	1%	CPN; CPN-1; CPN-2									x																												x	x
	CPE-13	1	Pck.-Grn. Alveolina	0%																																								
	CPE-12	1	Pck. Alveolina	0%																																								
	CPE-11	1	Pck. Alveolina	0%																																								
late Thanetian	CPE-10	5	Wck.-Pck. BF+Corals+Bryos+Distichoplax	10-20% Dispersed rhodos.							x	x							x	x	x			x				x	x	x	x						x		x	
	CPE-9	1	Wck. Solenomeris+Distichoplax	10-20%																										x	x	x	x	x							
	CPE-8	5	Flst. Rhodos.	20-25% Rhodolith bed			x		x			?							x	x	x	x			x				x	x	x	x	x					x		x	x
	CPE-7	2	Rud. BF+CCA	20-25%					x				x	x				x		x	x			x							x	x					x	x	x		x
	CPE-6	1	Pck. LBF+CCA	35-40%				x	x					x						x								x	x		x						x		x		
	CPE-5	7	Rud. BF+CCA+Mollusks+Corals	10-30%			x		x				x	x				x		x										x		x	x	x				x			x
	CPE-4	3	Rud. BF+CCA	5-15%																					x	x	x					x	x			x		x			x
	CPE-3	1	Pck. LBF+SBF+CCA	3-5%						x											x	x									x										
	CPE-2	1	Pck. LBF+SBF+serpulids+gastropods	3-5%																								x			x										
	CPE-1	2	Grn.-Pack. LBF+serpulids	< 1%																								x			x						x				
	Serraduy section																																											
early Ypresian	SEE-10	2	Calcareous sandstone	0%																																								
	SEE-9	2	Pck. Corals+Miliolids+CCA	1-3%																				x	x														x		x	
	SEE-8	3	Flst.(Frm.) Corals+CCA crusts+Miliolids	1-5%																x				x	x				x										x		x	x
	SEE-7	2	Flst.(Frm.) Corals+CCA crusts+Miliolids	3-5%			x	x						x						x					x				x										x		x	
	SEE-6	2	Pck. Corals+BF+CCA	5%							x			x			x							x	x			x	x					x	x			x		x	
	SEE-5	4	Pck. Corals+BF+CCA (crusts)	1-5%									x	x		x								x			x	x	x	x								x		x	
	SEE-4	2	Pck. Bioclastic	1-5%											x									x						x										x	x
	SEE-3	3	Grn. Bioclastic	< 1%																				x																x		
	SEE-2	1	Grn. Alveolina+Corals+BF	1-3%										x	x									x																x		
	SEE-1	2	Grn. Alveolina+Miliolids	< 1%																				x																x		
	SEW-3	4	Flst.(Frm.) Corals+CCA+Miliolids	1-3%										x			x	x		x			x						x	x									x	x	x
late Thanetian	SEW-2																																											
	SEW-1	8	Grn.-Pck. Corals+BF+CCA	20-50%			x		x			x		x				x		x	x	x		x					x	x	x	x					x	x	x	x		x
	SEW-0	2	Flst.(Frame.) Corals+Forams	1-3%							x	x					x								x						x											

Wck, Wackestone; Pck, Packstone; Grn, Grainstone; Rud, Rudstone; Flst, Floastone; F, Framestone; CCA, Crustose coralline algae; Bryos, Bryozoans; LBF, Larger benthic foraminifera; BF, Benthic foraminifera; Rhodos, Rhodoliths.

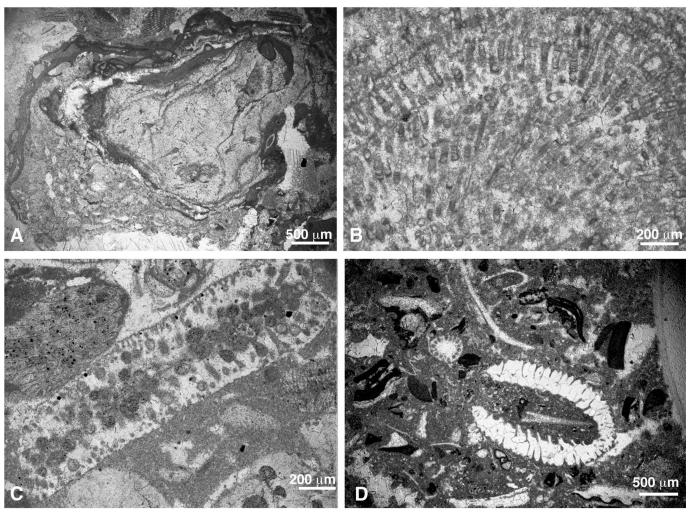

FIGURE 3 | **(A)** Superimposed thalli of *Polystrata alba* (nucleus of the rhodolith) and coralline algae (sample SEW-15). **(B)** *Marinella lugeoni* (sample CPE-7). **(C)** Longitudinal section of a *Halimeda* plate (sample CPE-5). **(D)** Oblique section of a dasycladalean green alga (sample SEE-6i).

Aguirre, 2004; Aguirre et al., 2017). Particularly interesting is the relative abundance of geniculate coralline algae, which dominate in high-energy intertidal, shallow-subtidal settings, both in the present day (Garbary and Johansen, 1982; Canals and Ballesteros, 1997; Couto et al., 2014) and in the fossil record (Scheibner et al., 2007; Quaranta et al., 2012; Brandano, 2017). In these settings, they are prone to disarticulation and breakage after death, thus, reducing their fossilization potential (Aguirre et al., 2000a; Aguirre et al., 2010; Basso, 2012). During the late Thanetian, coralline algae diversified in small coral buildups, such as those found in the Serraduy section (samples SEW-0 and SEW-1) (**Figures 2B**, **7**).

In addition to coralline algal fragments, loosely and densely packed rhodolith beds developed at the upper part of the Navarri Formation. Although rhodolith shape and algal growth forms in the outer parts of the rhodoliths can be water-depth and hydrodynamic indicators (Bracchi et al., 2022), laboratory experiments and field observations have shown that in most cases there is no correlation between those factors (Aguirre et al., 2017; Braga, 2017; O'Connell et al., 2020; and references therein). In the Campo section, several evidences suggest that rhodolith beds formed in relatively deep, calm marine settings, most likely in a middle ramp: 1) the matrix surrounding the rhodoliths is fine grained-muddy carbonate; 2) *Sporolithon* spp. are major components of the rhodoliths, indicating growth in relative deep waters (several tens of meters), as abundance of Sporolithales increases with water depth (Adey and Macintyre, 1973; Adey, 1979; Minnery et al., 1985; Adey, 1986; Fravega et al., 1989; Minnery, 1990; Aguirre et al., 2000a; Braga and Aguirre, 2001; Braga and Aguirre, 2004; Braga and Bassi, 2007; Braga et al., 2009); and, 3) geopetal fillings point to a normal polarity of rhodoliths and preservation in growth position without significant reworking.

The uppermost carbonate beds of the upper Thanetian Navarri Formation, immediately below the karst surface, are overwhelmingly dominated by large laminar thalli of *D. biserialis* dispersed in a muddy (packstone-wackestone) matrix (**Figure 8**). Loose laminar growth forms of this coralline alga in fine-grained sediments suggest low energy conditions. These sediments at the top of the Navarri Formation are interpreted as middle ramp deposits as well (Scheibner et al, 2007; Li et al., 2020).

In the Campo section, the Paleocene-Eocene boundary is represented by a subaerial erosional surface that reflects a profound paleoenvironmental change in the study region. Overlying the unconformity, continental clays, sands, and discontinuous palustrine limestones of the Claret Formation formed. Continental sedimentation was coeval with a sea level lowering during the carbon isotope excursion (CIE) recorded at the Paleocene/Eocene transition (e.g., Pujalte et al., 2014; Pujalte et al., 2022). In the Campo section, the continental interval is overlain by packstone-wackestone beds of alveolinids, which are topped, in turn, by laminated microbial carbonates (upper deposits of IL-1 sequence). The almost exclusive dominance of *Alveolina* indicates that they formed in a very restricted lagoon with probable fluctuations in salinity (BouDagher-Fadel, 2018). The profuse development of microbial laminites, with evaporite minerals, reveals marginal/very restricted to eventually hypersaline environmental conditions. Coralline algae were absent in all these settings. Stratal geometry of these first marine beds shows an onlap indicating relative sea-level rise, which increased accommodation.

Higher up into the study sections, milioliids and locally oysters (sample CPE-14), together with *Alveolina*, dominate the fossil assemblages. Milioliids are small benthic foraminifers preferentially inhabiting lagoons (Murray, 1991; Murray, 2006). Dasyclads are also abundant in the lower Ypresian carbonates, particularly in the Serraduy section (**Table 1**). They preferentially inhabit low latitude, shallow bays and lagoons (Flügel, 1985; Flügel, 1991; Berger and Kaever, 1992; Aguirre and Riding, 2005; Berger, 2006).

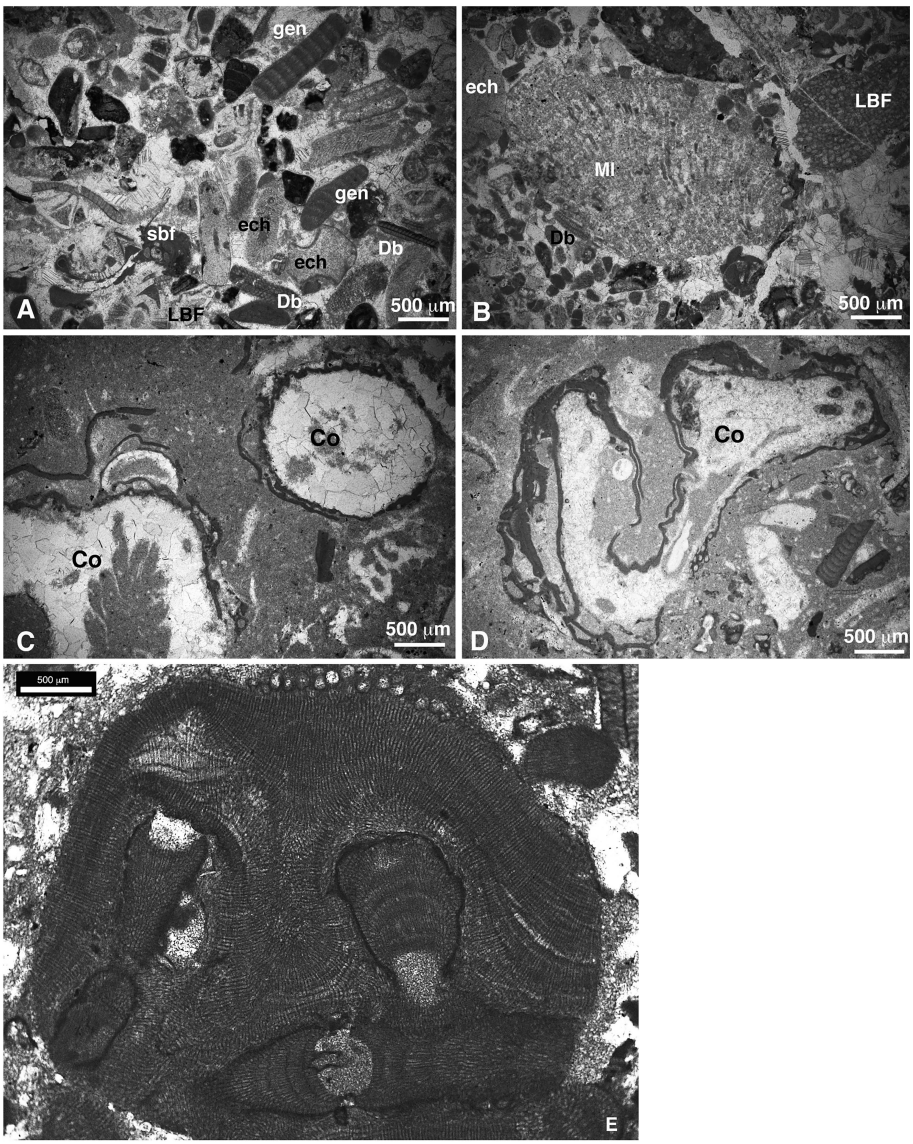

FIGURE 4 | **(A, B)** Grainstone-rudstones of bioclasts including geniculate coralline algae (gen), *D. biserialis* (Db), larger benthic foraminifera (LBF), echinoids (ech), small benthic foraminifera (sbf), and *M. lugeoni* (Ml) (A: sample CPE-4; B: sample CPE-7). **(C, D)** Thin laminar encrusting coralline algae coating corals (Co) embedded in a wackestone matrix (**C**: sample SEW-2ii; D: sample SEE-6). **(E)** *Sporolithon* sp. engulfing geniculate coralline algae (sample SEW-1ii).

Locally, small coral patches, corresponding to samples CPE-15 and CPN-3 of the Campo section, as well as samples SEW-3 and SEE-5—SEE-9 of the Serraduy section, grew in these shallow-water environments dominated by alveolinids. Corals are embedded in a wackestone-packstone matrix, very rich in milioliids, and suggest relatively normal marine conditions, probably in lagoonal areas with connection with open marine waters. The only records of corallines in the lower Ypresian deposits of the Campo section are found in the coral patches at the base of sequence IL-2. In the Serraduy section, coralline algae are present but scarce in all samples from the lower Ypresian IL-2 sequence, being more abundant in the coral buildups (**Table 1**).

In the Campo section, the lower Ypresian carbonates above the coral buildups represent a progressive deepening trend, as inferred by the progressive diversification of the larger benthic foraminifer assemblages (particularly, nummulitids) as well as other invertebrates (bivalves, gastropods, and echinoderms). In the uppermost part of the section, a monospecific bed of lucinids preserved in life position (below sample CPE-19) is found. The family Lucinidae is one of the most diversified groups of bivalves in chemosynthetic communities associated with hydrothermal vents and cold seeps, disoxic bottom conditions and/or eutrophic settings (Taylor and Glover, 2006). This suggests the prevalence of harsh conditions for coralline algae during the early Ypresian deepening in the Campo section.

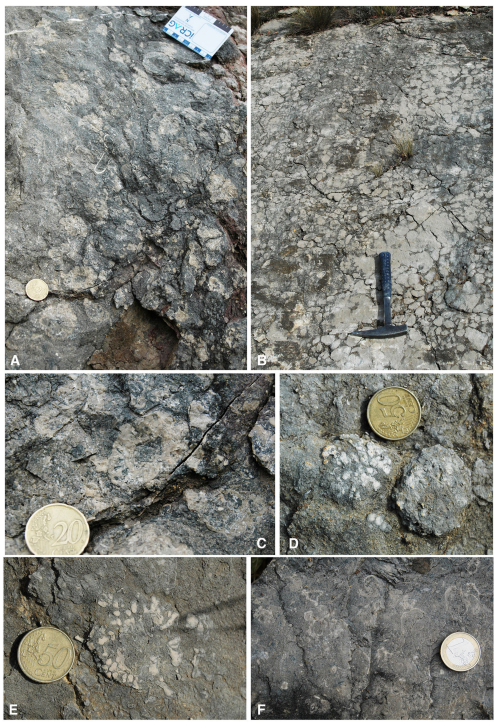

FIGURE 5 | **(A)** Loosely packed rhodolith bed. **(B)** Densely packed rhodolith bed. **(C–E)** Detail of warty-fruticose rhodliths. **(F)** Thin encrusting algae coating corals. **(A–E)**: pictures of the upper part of the Navarri Fm. (late Thanetian) in the Campo section. **(F)** picture of the lower part of the Serraduy Fm. (early Ypresian) in the Campo section.

Coralline Algal Diversity During the PETM

In terms of number of species, coralline algae maintain similar species richness along the late Thanetian-early Ypresian interval in our study case (**Figure 7**). During the Thanetian, diversity peaked in particular beds, such as the rhodolith beds of the Campo section and in the coral buildups of the Serraduy section. In addition, the three coralline algal groups, namely Sporolithales, Hapalidiales, and Corallinales, keep similar diversity values, being Corallinales and Hapalidiales the most diversified ones (**Figure 7**).

Our results also show that the species found in the early Ypresian are also found in the late Thanetian deposits (**Table 1**). This means that no extinction event is recorded at the Paleocene-Eocene transition at Campo and Serraduy sections. Furthermore, no significant turnover is observed since no new species occurred in the lower Ypresian deposits.

The global diversification history of coralline algae shows a slight increase in diversity during the late Paleocene-early Eocene transition due to the diversification of Hapalidiales (Aguirre et al., 2000a). Nonetheless, no significant diversity change is observed in the Pyrenean study areas. Both in Campo and Serraduy sections, coralline algae disappeared during the deposition of the Claret Formation and recovered long time after the Paleocene-Eocene boundary, within the Serraduy Formation.

After the continentalization during the PETM interval, represented by the Claret Formation, marine deposition restarted in the early Ypresian but in very restricted lagoonal settings, unfavorable for the growth of coralline algae (Woelkerling et al., 1993). These paleoenvironmental conditions remained during accumulation of *Alveolina*-rich deposits that form the bulk of the Serraduy Formation, inhibiting extensive coralline algal development. In the Campo section, siliciclastic content increases in the two topmost samples (CPE-19 and CPE-20) representing the inner to middle ramp transition. This might account for the virtual absence of coralline algae since terrigenous supply inhibits their profuse development (Aguirre et al., 2017).

Coralline algae, however, occurred associated with the lower Ypresian coral patch reefs, as laminar and thin crusts coating the coral colonies (**Figures 4C, D**, **5F**). Coral growth and expansion of coralline algae denote the reestablishment of fully marine conditions. In these settings, coralline algae became totally diversified, with species richness similar to that of the late Thanetian (**Table 1**; **Figure 7**). It seems, therefore, that, in the Pyrenean localities, coralline algae disappeared after the PETM due to drastic shifts in local environmental conditions, not as a consequence of global events.

We are not able to ascertain that the massive release of CO_2 to the atmosphere ~55.6 Ma, with the consequent ocean acidification due to lowering pH and temperature rise, affected negatively to coralline algae. Indeed, species richness and species composition were the same when fully marine conditions resumed in the region.

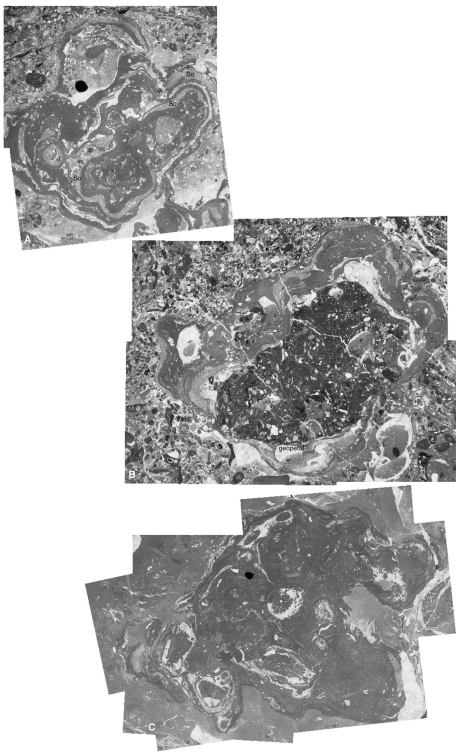

FIGURE 6 | Composite pictures of three rhodoliths. **(A)** Rhodolith formed by the intergrowth of encrusting coralline algae and *Solenomeris* (So) embedded in a packstone matrix (sample CPE-8iii). **(B)** Encrusting-warty thalli of *Sporolithon* spp. overgrowing a lithified carbonate nucleus. Geopetal filling, coinciding with the asymmetrical algal development to the upper part of the picture, is indicated in the lower part of the photo (sample CPE-8). **(C)** Laminar-encrusting algae overgrowing corals. The rhodolith is embedded in a wackestone-mudstone marly matrix (sample CPE-10).

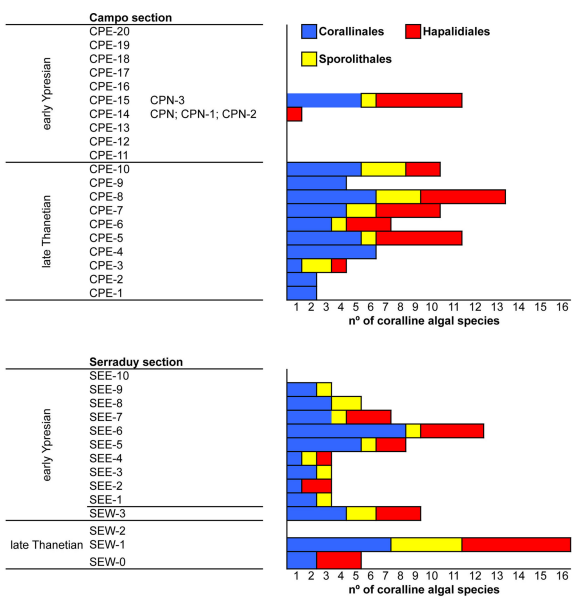

FIGURE 7 | Coralline algal species abundance in the study sections.

Furthermore to analyze inventories of coralline algal species to evaluate diversity changes throughout the Paleocene-Eocene transition, it is also interesting to investigate the PETM effects on rhodolith beds. After the mass extinction affecting coralline algae at the end of the Cretaceous (Aguirre et al., 2000a; Aguirre et al., 2000b), rhodolith beds spread significantly during the late Danian and early Thanetian (Aguirre et al., 2007); i.e., after a long time of recovery. In the Pyrenees, rhodolith beds were present by the end of the Thanetian (uppermost interval of Navarri Formation) but they were absent during the early Ypresian. Globally, a significant reduction of rhodolith-rich deposits, which are rarely recorded, took place during the early Eocene (Howe, 1934; Lemoine and Mengaud, 1934; Aguirre et al., 2011), and continued during the middle Eocene, at least in mid and high latitudes (Aguirre et al., 2020). Rhodolith beds became widely recorded again in the late Eocene (Aguirre et al., 2020).

CONCLUSIONS

We studied coralline algal assemblages in shallow-marine carbonate and siliciclastic deposits during the Paleocene/Eocene

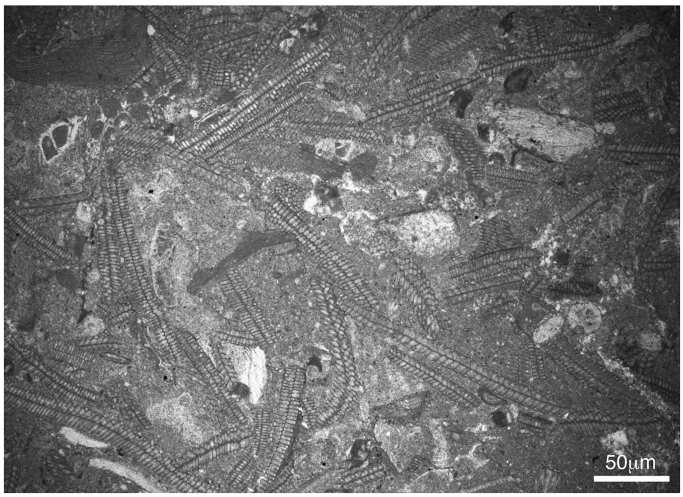

FIGURE 8 | *Disctichoplax biserialis* concentration at the upper part of the Navarri Formation (late Thanetian) in the Campo section (sample CEP-9).

Thermal Maximum (PETM) in the Campo and Serraduy sections, in the south-central Pyrenees (Huesca, N Spain). Coralline algae occur mostly as fragments of branches and forming rhodoliths, which occur either dispersed or in densely packed concentrations (rhodolith beds). Representatives of the orders Sporolithales, Hapalidiales, and Corallinales are present, being Corallinales and Hapalidiales the most diversified ones. Species composition and diversity do not change throughout the Paleocene/Eocene boundary but the relative abundance of coralline algae as components of the carbonate sediments underwent a considerable reduction: from abundant during the late Thanetian to scarce during the early Ypresian. This abundance drop was due to a drastic change in the local paleoenvironmental conditions immediately after the Paleocene/Eocene boundary. The Thanetian marine sedimentation ended with a hardground, which is followed, in turn, by continental deposits formed during the PETM. Marine deposition resumed in shallow, very restricted lagoon and peritidal settings, as indicated by the almost exclusive dominance of *Alveolina*, milioliids and soritids in muddy carbonates. These paleoenvironmental conditions were unfavorable for the development of coralline algae. They reappeared, and were locally abundant, associated with corals in lower Ypresian beds, where they show diversity values and species composition similar to pre-PETM deposits.

TAXONOMIC APPENDIX

Species identification of fossil specimens is always challenging since it is based on morpho-anatomical features and depends mostly on their preservation state. Concerning fossil coralline algae, taking into consideration the ongoing phylogenetic classification schemes of recent taxa, their identification is complicated even at supraspecific levels. Preservation of the sporangial reproductive structures is needed to assign fossil specimens to any of the four fully-calcified coralline algal orders (Jeong et al., 2021). Unfortunately, this is not always the case and many fossil specimens cannot be correctly identified at any supraspecific level. Based on characters usually preserved in the fossil record, the most feasible taxonomic approach is, at best, the subfamily or family level. The problem is exacerbated when trying to use an already proposed species epithet based on fossil material. Historically, authors have defined species based on ambiguous anatomical characters and have preferred to proposed new names for their findings instead of using already existing ones (Braga and Aguirre, 1995; Aguirre and Braga, 2005). An additional trouble is the inconsistent use of published species names by other scientists to name their specimens. This has produced an overabundance of species names to designate entities that cannot be unambiguously separated (Aguirre and Braga, 2005).

Regarding our study case, we checked species names of coralline algae described in Paleocene-Oligocene deposits. To avoid reinterpretations of original species definitions by later authors, we resort to the original descriptions and illustrations of the species. A description of the anatomical and reproductive features of some coralline algal species recognized in our samples and their similarities with closest species are given below. We focus only on those species that deserve some discussion since they underwent diverse taxonomic interpretations. Thus, we discuss the possible species names that can be assigned to some of the identified morphospecies. For those specimens that are not easily attributed to any species name, we keep an open species nomenclature. In addition, we provide a taxonomic key for all the identified species (**Table 2**) and illustrate all of them in **Figures 9**–**12**.

Order Sporolithales (**Figures 9A–E**)

1. *Sporolithon lugeonii* (Pfender) Ghosh and Maithy 1996 (**Figures 9D, E**) We have identified some plants with small

TABLE 2 | Identification key with the anatomical and reproductive features characterizing the genera and species found in the study areas.

1. Sporangial compartments	**Sporolithales**
1. Multiporate sporangial conceptacles	**Hapalidiales**
1. Uniporate sporangial conceptacles	**Corallinales**
Sporolithales	
1. Few sporangial cavities per sori	2
2. Sporangial compartments 65-75 μm in height	3
3. Ovoid sporangial cavities in section; diameter = 40-50 μm, high = 70-75 μm	*Sporolithon* cf. *oulianovii* Pfender 1926
3. Sporangial cavities in nemathecium-like protruding sori	*Sporolithon* sp. 1
3. Rectangular sporangial cavities in section; 65-70 μm in height	*Sporolithon brevium* (Me.Lemoine) Jul.Aguirre & J.C.Braga 1998/*S. airoldii* (Fravega) Vannucci, Quaranta & Basso 2010
1. Numerous sporangial cavities per sori	4
4. Sporangial cavities rectangular in section and narrow; diameter = 40-50 μm, high = 70-90 μm	*Sporolithon lugeonii* (Pfender) Ghosh and Maithy 1996
Hapalidiales	
1. Thallus dimerous	*Melobesia* sp.
1. Thallus monomerous	2
2. Warty to fruticose thalli	3
3. Rectangular sporangial conceptacles in section	*Lithothamnion camarasae* Pfender 1926
3. Large rectangular-polygonal cells with no lateral alignment of cells in adjacent filaments; thick cell walls	*Lithothamnion* cf. *corallinaeforme* Me.Lemoine, 1924
3. Non-protruding, flat sporangial conceptacles (up to 750 μm in diameter and 100 μm in height).	*Lithothamnion concretum* M.Howe, 1919a
3. Regularly zonate thallus; slightly protruding sporangial conceptacles <200 μm in diameter	*Lithothamnion* cf. *exuberans* Mastrorilli, 1967
3. Regularly-irregularly zonate thallus; sporangial conceptacles > 400 μm with high pore canals.	*Lithothamnion vaughani* M.Howe, 1919b
3. Non-zonate thallus; slightly protruding sporangial conceptacles 200 μm-260 μm in diameter	*Lithothamnion* sp. 1
3. Groups of protruding sporangial conceptacles piled up in warts	*Lithothamnion* sp. 2
2. Thin encrusting thalli	4
4. Protruding sporangial conceptacles isolated in the thallus	*Lithothamnion crispithallus* J.H.Johnson, 1957
4. Protruding sporangial conceptacles >400 μm in diameter	*Lithothamnion* sp. 3
4. Sporangial conceptacles 200-400 μm in diameter	*Lithothamnion* sp. 5
4. Sporangial conceptacles < 200 μm in diameter	*Lithothamnion* sp. 4
Corallinales	
1. Geniculate thallus	2
2. Palisade-like medullar cells; medullar region made up to 13 tiers of cells	*Jania nummulitica* Me.Lemoine, 1928
2. Sporangial conceptacle in a terminal position in the intergeniculum	Geniculate sp. 1, cf. *Corallina prisca* J.H.Johnson, 1957
2. Sporangial conceptacle surrounded by lateral branches	Geniculate sp. 2
2. Sporangial conceptacle in lateral position	Geniculate sp. 3
1. Non-geniculate thallus	3
3. Thallus dimerous	4
4. Ventral layer of polygonal-irregular cell filaments	*Karpathia sphaerocellulosa* Maslov 1962
4. Ventral layer of quadrangular cells	*Hydrolithon lemoineii* (Miranda) Jul.Aguirre, J.C.Braga, Bassi 2011
4. Large, rectangular ventral palisade cell filaments; small dorsal cells	*Lithoporella melobesioides* (Foslie) Foslie 1909
4. Single layer of rectangular-quadrangular, non-palisade ventral cells with small, cap-like epithallial cells	*Lithoporella minus* J.H.Johnson, 1964
3. Thallus monomerous	5
5. Isobilateral organization of the ventral filaments	*Distichoplax biserialis* Dietrich 1927
5. Plumose ventral core	6
6. Encrusting thalli	*Spongites* sp. 3
6. Warty and fruticose thalli	7
7. Highly protruding sporangial conceptacles with eccentric, large pore canal	*Spongites* sp. 1
7. Slightly protruding sporangial conceptacle	*Spongites* sp. 2

uniporate, pear-like shaped conceptacles (100-125 μm in diameter and 100 μm in height) (**Figure 9E**). They show vegetative anatomy and cell sizes similar to *Sporolithon lugeonii*. Therefore, we interpret these plants as gametangial (male) conceptacles of *S. lugeonii*. Nonetheless, these gametangial conceptacles coincide both in shape and size to those described as *Sporolithon* sp. 2 by Basso et al. (2019) or as *S. airoldii* by Vannucci et al. (2010).

2. *Sporolithon brevium* (Lemoine) Aguirre and Braga 1988/ *Sporolithon airoldii* (Fravega) Vannucci, Quaranta and Basso 2010 (**Figure 9C**). Based on vegetative anatomy, thallus construction and reproductive structures, this species shows similarities with *Sporolithon airoldii* (Fravega, 1984; Vannucci et al., 2010). It also recalls the type material of *Sporolithon brevium* (Aguirre and Braga, 1998), and *Sporolithon keenani* Howe 1934.

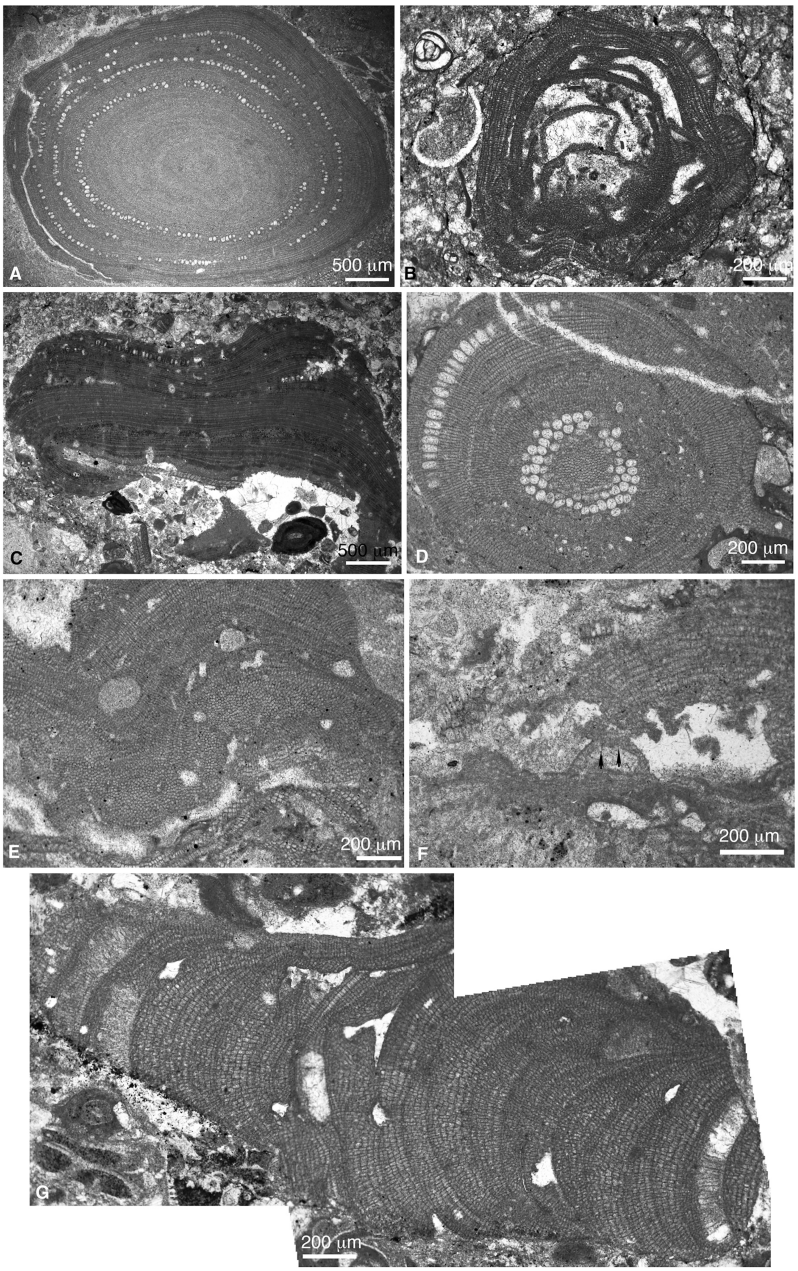

FIGURE 9 | **(A)** *Sporolithon oulianovii* (sample CPE-10). **(B)** *Sporolithon* sp. 1 (sample CPN-3). **(C)** *Sporolithon brevium/airoldii* (sample CPE-3). **(D)** *Sporolithon lugeonii* (sample CPE-8). **(E)** Spermetangial conceptacles of *S. lugeonii* (sample CPE-8). **(F)** *Melobesia* sp. Arrowheads indicacte two pore canals at the conceptacle roof (sample CPE-8). **(G)** Branch of *Lithothamnion* cf. *corallioides* (sample CPE-6).

3. *Sporolithon* sp. 1 (**Figure 9B**). This species has been found in one sample. It is a monomerous plant with a laminar and encrusting growth form. Thallus is thin, with a thin plumose ventral core, made up by 2-3 cell rows that bend upwards to the peripheral region, which consists of up to 15 cell rows. Reproductive structures consist of a few isolated sporangial cavities (3-5 cavities) grouped into very protruding nemathecia-like sori.
4. Undifferentiated Sporolithales. Under this category, we include small unidentifiable fragments of plants preserving sori.

Order Hapalidales (**Figures 9F, G**, **10**, **11A–C**).

1. *Melobesia* sp. (**Figure 9F**). This species shows dimerous, laminar, very thin thalli made up of 2-3 cell rows that thicken around multiporate conceptacle cavities. The study specimens show similarities with *Melobesia* sp. from the

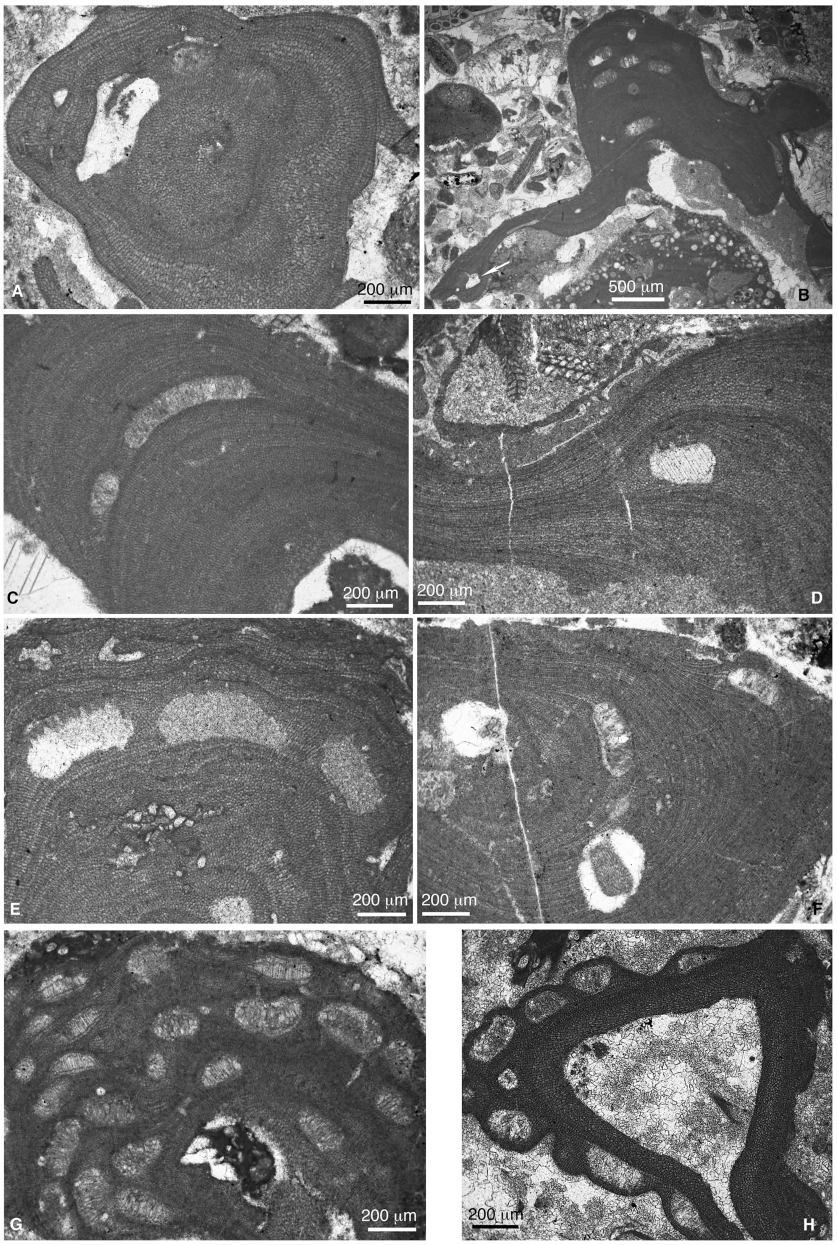

FIGURE 10 | **(A)** Spermatangial conceptacle of *Lithothamnion* cf. *corallioides* (sample CPE-6). **(B)** *Lithothamnion camarasae* (sample CPE-6). **(C)** *Lithothamnion concretum* (sample SEW-1). **(D)** *Lithothamnion* cf. *exhuberans* (sample CPE-15). **(E)** *Lithothamnion vaughanii* (sample SEW-1). **(F)** *Lithothamnion* sp. 1 (sample CPE-7). **(G)** *Lithothamnion* sp. 2 (sample SEE-2). **(H)** *Lithothamnion crispithallus* (sample SEE-6).

middle Eocene from the Subbetic of the Betic Cordillera (S Spain) (Aguirre et al., 2020).

2. *Lithothamnion concretum* Howe 1919a (**Figure 10C**). The study material fits with the original description of this species by Howe (1919a). That is, fruticose plants, occasionally encrusting, with cell filaments arranged in regular zones in the center of the branches, with a relatively well-defined lateral alignment of cells of adjacent filaments. Sporangial conceptacles are up to 750 μm in diameter and 100 μm in height and do not protrude on the thallus surface. This species is close to *Lithothamnion pianfolchi* Mastrorilli, 1967 and that identified as *Mesophyllum ryukyuensis* Johnson, 1964. Nonetheless, these two species have smaller sporangial conceptacles. The species also resembles *Lithothamnion ramosissimum* (Reuss) Piller 1994 (Piller, 1994; Aguirre et al., 1996), although this species is more recent (Neogene).
3. *Lithothamnion* cf. *corallinaeforme* Lemoine 1924 (**Figures 9G**, **10A**). The specimens identified within this

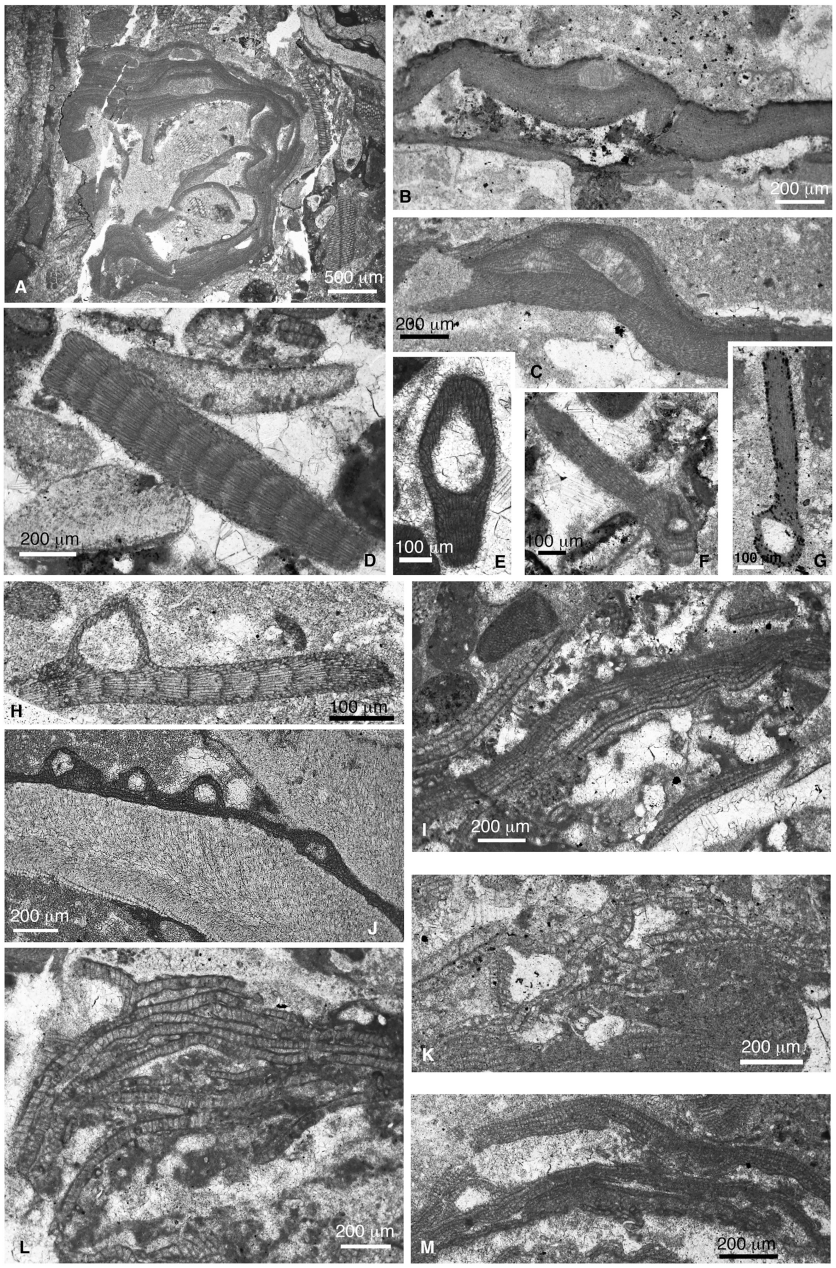

FIGURE 11 | **(A)** *Lithothamnion* sp. 3 (sample CPE-15). **(B)** *Lithothamnion* sp. 4 (sample SEE-5i). **(C)** *Lithothamnion* sp. 5 (sample SEW-3ii). **(D)** *Jania nummulitica* (sample CPE-4i). **(E)** Geniculate sp. 1 (cf. *Corallina prisca*) (sample CPE-4). **(F)** Geniculate sp. 2 [sample (CPE-4ii)]. **(G)** Geniculate sp. 2 (sample SEE-5i). **(H)** Geniculate sp. 3 (sample SEE-6i). **(I)** *Karpathia sphaerocellulosa* (sample CPE-5iii). **(J)** *Hydrolithon lemoineii* (sample SEE-6i). **(K)** *Lithoporella minus* (sample SEW-1i). **(L)** *L. minus* showing a uniporate sporangial conceptacle partially preserved (sample CPE-8iii). **(M)** *Lithoporella melobesioides* (sample CPE-10iii).

species epithet show growth form, thallus construction, vegetative anatomy and reproductive structures comparable with the type material of *L. corallinaeforme* Lemoine, 1924 as reassessed by Aguirre et al. (2012). *Lithothamnion marianae* Johnson, 1957 presents similarities with Lemoine's species. The growth forms (slender, long branches), as well as the cell size and shape (rectangular to polygonal with a thickened cell wall) are anatomical features highlighted both by Johnson (1957) and by Aguirre et al. (2012) in the description of the two species.

4. *Lithothamnion* cf. *exuberans* Mastrorilli 1967 (**Figure 10D**). This species occurs as fragmented branches. Cell filaments in the center of the branch form regular growth zones. Sporangial conceptacles slightly protrude above the thallus

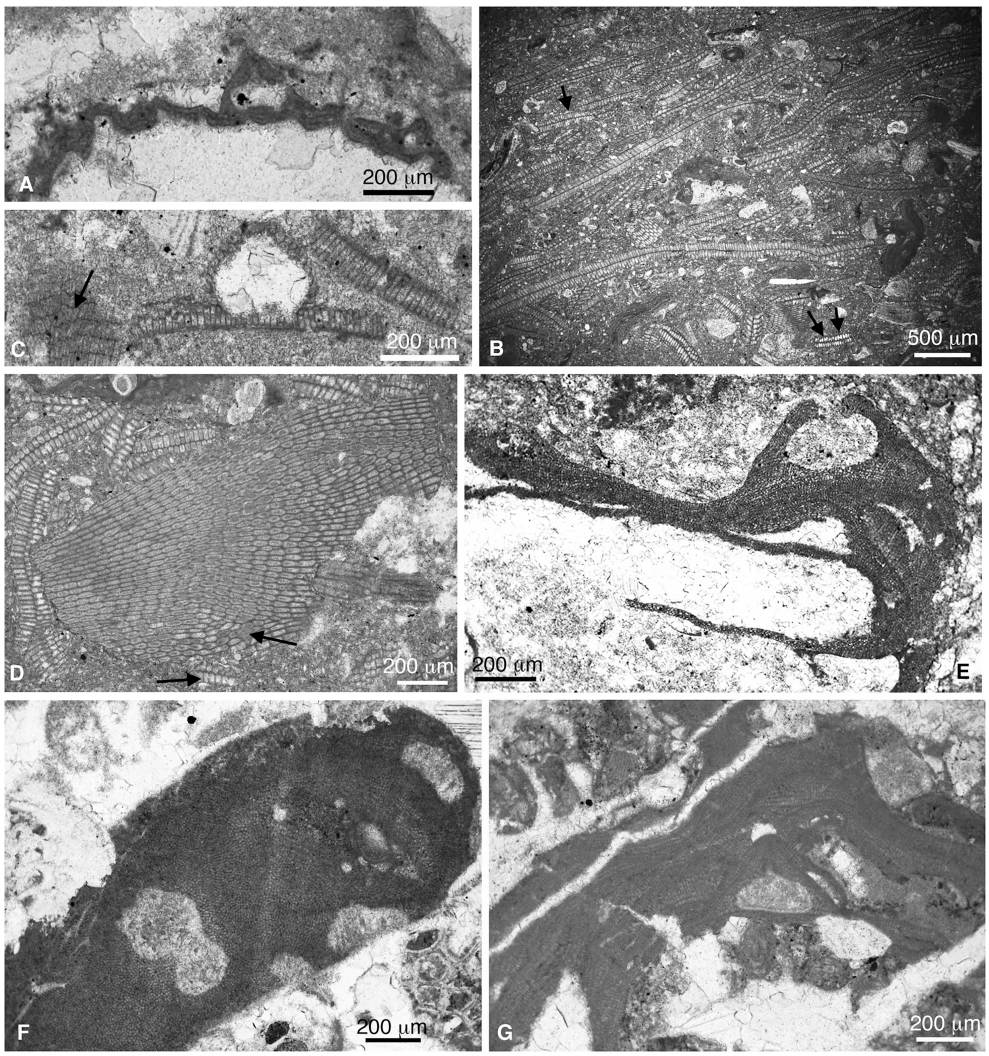

FIGURE 12 | **(A)** *Lithoporella melobesioides* (sample SEW-3ii). **(B)** Laminar thalli of *Distichoplax biserialis* in a wackestone matrix (sample CPE-9). Arrows mark cell fusions. **(C)** *D. dbiserialis* showing a uniporate sporangial conceptacle (sample SEE-9). Arrow marks cell fusions. **(D)** Oblique section of a lamina of *D. biserialis* (sample CPE-9). Arrows mark cell fusions. **(E)** *Spongites* sp. 3 (sample CPN-3). **(F)** *Spongites* sp. 2 (sample CPN-5ii). **(G)** *Spongites* sp. 1 (sample CPE-7).

surface and measure about 200 μm in diameter and 100-130 μm in height. They are slightly trapezoidal but irregular in shape and possess conspicuous pore canals in the roof. The specimens showing these features can be assigned to the species *Lithothamnion exuberans* Mastrorilli, 1967, who highlighted the irregular shape of the sporangial conceptacles, which is a typical character of the study material. Similar coralline algae were described as *Lithothamnion* sp. 4 by Aguirre et al. (2020) from the middle Eocene carbonates of Subbetic Zones, Betic Cordillera (S Spain), Colombia, and Dominican Republic.

5. *Lithothamnion crispithallus* Johnson 1957 (**Figure 10H**). Thin thallus with a well-developed plumose ventral core and a thin peripheral region, which thickens substantially surrounding conceptacles. Sporangial conceptacles, which are crowded in portions of the thallus, protrude on the thallus surface generating a wart-like structure. They are rectangular or dome-like in shape ranging from 190 μm to 250 μm in diameter and from 100 μm to 140 μm in height. This alga occurs attached to hard skeletons or as crusts isolated in the sediment. Johnson (1957) highlighted the crowding of the conceptacles as characteristic of the species. *Lithothamnion charollaisi* Segonzac and Charollais 1974 shows similarities with *L. crispithallus*. Nonetheless, the description of the species is very limited precluding feasible comparisons.
6. *Lithothamnion vaughani* Howe 1919b (**Figure 10E**). In the protologue of this species, Howe (1919b) indicated "primary hypothallia somewhat reduced, …. rather irregularly arranged (i.e., not distinctly "coaxial")" (Howe, 1919b; p. 6).

Later, Lemoine (1928; see also Lemoine, 1939) transferred the species to the new genus *Mesophyllum* that she described: "Les espèces fossiles qui me paraissent faire partie du genre *Mesophylllum* sont: … *M. vaughani* Howe" (Lemoine, 1928; p. 253). This new genus attribution has been followed by later authors. Nonetheless, taking into consideration the clear reference to the plumose ventral core we keep the original genus attribution by Howe (1919b).

7. *Lithothamnion* sp. 2 (**Figure 10G**). This species occurs as fruticose or encrusting plants with branches showing irregular internal zones. The most characteristic feature is that numerous multiporate sporangial conceptacles are grouped in the tips of branches or warts. They are mostly secondarily filled by adventitious cells. Thallus morphology, internal organization, conceptacle shapes and sizes, and their distribution allow comparing this species with *Mesophyllum schenckii* Howe, 1934, *Lithothamnion wallisium* Johnson and Tafur, 1952, later figured by Johnson and Stewart (1953), and *Lithothamnion* sp. Stockar (2000). It also shows certain resemblance with *Mesophyllum galettoi* Mastrorilli, 1967. Members of the genus *Mesophyllum* present a predominantly coaxial hypothallus. Nonetheless, in the protologue of *M. schenckii* and *M. galettoi*, both Howe (1934) and Mastrorilli (1967), respectively, indicate the presence of a plumose ventral core. The specimens we have studied show plumose ventral core, so, we assign them to *Lithothamnion*.

   One specimen in sample SEW-1 shows a large triangular conceptacle with a long single pore in the roof. The pore canal protrudes above the thallus surface generating a wart-like protuberance. This alga shows the same growth morphology and thallus organization as that of *Lithothamnion* sp. 2, thus, we interpret it as a gametangial plant of the species.
8. Undifferentiated Hapalidiales. Under this category, we include small unidentifiable fragments of encrusting thalli with well-developed plumose hypothallus and a thin perithallus, which thickens around sporangial multiporate conceptacles.

   Order Corallinales (**Figures 11D–M**, **12**)

1. Geniculate sp. 1 (**Figure 11E**). It occurs as calcified disarticulated portions of intergenicula with cell fusions. One portion presents a uniporate conceptacle located in a terminal position of the intergeniculum (**Figure 11E**). Fragmentation precludes genus identification; however, preserved features remind those of *Corallina prisca* Johnson, 1957 from the late Eocene of Saipan (Mariana Islands).
2. Geniculate sp. 2 (**Figures 11F, G**). Dispersed fragments of portions of calcified intergenicula with cell fusions. Two of these intergenicula preserve uniporate conceptacles in the terminal position that are surrounded by lateral branches. One of the specimens show a small conceptacle with a high pore canal (**Figure 11F**) and the other is bigger with a short pore canal (**Figure 11G**). The former is tentatively interpreted as a possible gametangial conceptacle of the same taxon.
3. Geniculate sp. 3 (**Figure 11H**). A single thallus showing cell fusions and a big uniporate sporangial conceptacle derived from cortical cells in a lateral position of the intergeniculum.
4. *Distichoplax biserialis* Dietrich 1927 (**Figures 12B–D**). This is a widely known species, although its attribution has been debated. In the study material, we have found laminar thalli of *D. biserialis* showing both conceptacle primordia and void uniporate sporangial conceptacles (**Figure 12C**), enabling the assignment of this species to the order Corallinales. Similar reproductive structures have been figured by Kiej (1963; 1964) and Dieni et al. (1979). Recently, Sarkar (2018) included this species within the subfamily Lithophylloideae, based on the absence of cell fusions, an interpretation also erroneously made by Aguirre et al. (2010). This species shows evident cell fusions, although they are sometimes nearly absent in some portions of the thallus (**Figures 12C, D**). Therefore, it cannot be considered a lithophylloid any longer (Rösler et al., 2017; Peña et al., 2020b). Athanasiadis (1995) already questioned the attribution of *Distichoplax* to Lithophylloideae and proposed its affinity with *Mastophora* or *Lithoporella.*
5. *Spongites* sp. 1 (**Figure 12G**). This species is relatively frequent in the study material. It occurs as crusts or broken branches and is characterized by uniporate sporangial conceptacles that show slightly eccentric pore canals in the conceptacle roof. (**Figure 12G**). The eccentric pore canal is highlighted by Stockar (1997) while describing what he identified as *Lithophyllum atrum* Conti 1945. Nonetheless, Conti (1945) did not mention this feature in the original description of the species. Furthermore, sporangial conceptacles of *L. atrum* are much bigger than those found in the present study. Based on the vegetative anatomy and the reproductive structures, additional names that fit with our material are those originally described as *Lithophyllum vicetinum* Mastrorrilli, 1973 or *Lithophyllum ligusticum* Airoldi, 1932. Vannucci (1970) figured a specimen identified as *Lithophyllum ligusticum* showing a uniporate sporangial conceptacle with an eccentric pore canal. The reassessment of the Airoldi's type material by Vannucci et al. (2008) led them to synonymize *L. ligusticum* and *Lithophyllum perrandoi*, Airoldi 1932 favoring the latter as the valid species name. Airoldi (1932) described a coaxial ventral core, the same thallus organization that can be observed in Figure (**1A** and **Figure 4**) of Vannucci et al. (2008). Nonetheless, these authors described the type material as having a plumose ventral core (their **Figure 2**).
6. *Spongites* sp. 2 (**Figure 12F**). Fragment of a fruticose plant obliquely cut showing numerous cell fusions. At the tip of the branch, a uniporate conceptacle, 270 μm in diameter and 110 μm in height, is observed. The pore canal is partially visible.
7. *Spongites* sp. 3 (**Figure 12E**). Thin encrusting monomerous plant with thin ventral core and peripheral region. The latter thickens around a protruding uniporate conceptacle 310 μm in diameter and 115 μm in height (**Figure 12E**). Conceptacle shape and size remember *Lithophyllum bassanense* Mastrorrilli, 1973.

8. Undifferentiated Corallinales. Fragments of coralline algae that show cell fusions and uniporate sporangial conceptacles but that do not show enough features to assign them to any species.

DATA AVAILABILITY STATEMENT

The original contributions presented in the study are included in the article/supplementary material. Further inquiries can be directed to the corresponding author.

AUTHOR CONTRIBUTIONS

All authors contributed to the article and approved the submitted version.

FUNDING

JA and JCB were funded by the research project PGC2018-099391-B-100 of the Spanish Ministerio de Ciencia e Innovación and by the Research Group RNM-190 of the Junta de Andalucía. JIB acknowledges funding through the Research Group IT930-16 of the Basque Government Research Programme.

REFERENCES

Adey, W. H. (1979). "Crustose Coralline Algae as Microenvironmental Indicators in the Tertiary," in *Historical Biogeography, Plate Tectonics and the Changing Environment*. Eds. J. Gray and A. J. Boucot (USA:Oregon State Univ. Press, Corvallis), 459–464.

Adey, W. H. (1986). "Coralline Algae as Indicators of Sea-Level," in *Sea-Level Research: A Manual for the Collection and Evaluation of Data*. Ed. van de Plassche, (Netherlands: Free Univ. Amsterdam), 229–280.

Adey, W. H., and Macintyre, I. G. (1973). Crustose Coralline Algae: A Re-Evaluation in the Geological Sciences. *Geol. Soc Am. Bull.* 84, 883–904. doi: 10.1130/0016-7606(1973)84<883:CCAARI>2.0.CO;2

Aguirre, J., Baceta, J. I., and Braga, J. C. (2007). Recovery of Marine Primary Producers After the Cretaceous-Tertiary Mass Extinction: Paleocene Calcareous Red Algae From the Iberian Peninsula. *Palaeogeogr. Palaeoclimatol. Palaeoecol.* 249, 393–411. doi: 10.1016/j.palaeo.2007.02.009

Aguirre, J., Bassi, D., and Braga, J. C. (2011). Taxonomic Assessment of Coralline Algal Species (Rhodophyta; Corallinales and Sporolithales) Described by Pfender, Lemoine, and Miranda From Northern Spain Type Localities. *Ann. Naturhist. Mus. Wien Ser. A* 113, 267–289.

Aguirre, J., and Braga, J. C. (1998). Redescription of Lemoine's, (1939) Types of Coralline Algal Species From Algeria. *Palaeontology* 41, 489–507.

Aguirre, J., and Braga, J. C. (2005). The Citation of Nongeniculate Fossil Coralline Red Algal Species in the Twentieth Century Literature: An Analysis With Implications. *Rev. Esp. Micropaleontol.* 37, 57–62.

Aguirre, J., Braga, J. C., and Bassi, D. (2017). "Rhodoliths and Rhodolith Beds in the Rock Record," in *Rhodolith/Maërl Beds: A Global Perspective*. Eds. R. Riosmena-Rodríguez, W. Nelson and J. Aguirre (Basel, Switzerland: Springer Intern. Publ.), 105–138.

Aguirre, J., Braga, J. C., Martín, J. M., and Betzler, C. (2012). Palaeoenvironmental and Stratigraphic Significance of Pliocene Rhodolith Beds and Coralline Algal Bioconstructions From the Carboneras Basin (SE Spain). *Geodiversitas* 34, 115–136. doi: 10.5252/g2012n1a7

Aguirre, J., Braga, J. C., and Piller, W. E. (1996). Reassessment of *Palaeothamnium* Conti 1946 (Corallinales, Rhodophyta). *Rev. Palaeobot. Palynol.* 94, 1–9. doi: 10.1016/S0034-6667(96)00013-9

Aguirre, J., Braga, J. C., Pujalte, V., Orue-Etxebarria, X., Salazar-Ortiz, E., Rincón-Martínez, D., et al. (2020). Middle Eocene Rhodoliths From the Tropical and Mid-Latitude Regions. *Diversity* 12, 117. doi: 10.3390/d12030117

Aguirre, J., Perfectti, F., and Braga, J. C. (2010). Integrating Phylogeny, Molecular Clocks and the Fossil Record in the Evolution of Coralline Algae (Corallinales, Rhodophyta). *Paleobiology* 36, 519–533. doi: 10.1666/09041.1

Aguirre, J., and Riding, R. (2005). Dasycladalean Algal Biodiversity Compared With Global Variations in Temperature and Sea Level Over the Past 350 Myr. *Palaios* 20, 581–588. doi: 10.2110/palo.2004.p04-33

Aguirre, J., Riding, R., and Braga, J. C. (2000a). Diversity of Coralline Red Algae: Origination and Extinction Patterns From the Early Cretaceous to the Pleistocene. *Paleobiology* 26, 651–667. doi: 10.1666/0094-8373(2000)026<0651:DOCRAO>2.0.CO;2

Aguirre, J., Riding, R., and Braga, J. C. (2000b). Late Cretaceous Incident Light Reduction: Evidence From Benthic Algae. *Lethaia* 33, 205–213. doi: 10.1080/00241160025100062

Airoldi, M. (1932). Contributo Allo Studio Delle Corallinacee Del Terziario Italiano. I – Le Corallinacee Dell'Oligocene Ligure-Piemontese. *Paleontogr. Ital.* 33, 55–83.

Alegret, L., Ortiz, S., Arenillas, I., and Molina, E. (2005). Paleoenvironmental Turnover Across the Paleocene/Eocene Boundary at the Stratotype Section in Dababiya (Egypt) Based on Benthic Foraminifera. *Terra Nova* 17, 526–536. doi: 10.1111/j.1365-3121.2005.00645.x

Alegret, L., Ortiz, S., and Molina, E. (2009b). Extinction and Recovery of Benthic Foraminifera Across the Paleocene–Eocene Thermal Maximum at the Alamedilla Section (Southern Spain). *Palaeogeogr. Palaeoclimatol. Palaeoecol.* 279, 186–200. doi: 10.1016/j.palaeo.2009.05.009

Alegret, L., Ortiz, S., Orue-Etxebarria, X., Bernaola, G., Baceta, J. I., Monechi, S., et al. (2009a). The Paleocene–Eocene Thermal Maximum: New Data on Microfossil Turnover at the Zumaia Section, Spain. *Palaios* 24, 318–328. doi: 10.2110/palo.2008.p08-057r

Anthony, K. R. N., Kline, D. I., Diaz-Pulido, G., Dove, S., and Hoegh-Guldberg, O. (2008). Ocean Acidification Causes Bleaching and Productivity Loss in Coral Reef Builders. *Proc. Nat. Acad. Sc.* 105, 17442–17446. doi: 10.1073/pnas.0804478105

Arostegi, J., Baceta, J. I., Pujalte, V., and Carracedo, M. (2011). Late Cretaceous—Palaeocene Mid-Latitude Climates: Inferences From Clay Mineralogy of Continental-Coastal Sequences (Tremp-Graus Area, Southern Pyrenees, N Spain). *Clay Min.* 46, 105–126. doi: 10.1180/claymin.2011.046.1.105

Athanasiadis, A (1995). Morphology, Anatomy and Reproduction of the Eastern Mediterranean Coralline Tenarea Tortuosa and Its Relationship to Members of the Lithophylloideae and Mastophoroideae (Rhodophyta, Corallinales). *Nordic J. Bot* 15, 655–63.

Baccelle, L., and Bosellini, A. (1956). Diagrammi Per La Stima Visiva Della Composizione Percentuale Nelle Rocche Sedimentary. *Ann. Univ. Ferrara (Nuova Ser.) Sez. 9 Sc. Geol. Paleontol.* 1, 59–62.

Baceta, J. I. (1996). "El Maastrichtiense Superior, Paleoceno E Ilerdiense Inferior De La Región Vasco-Cantábrica: Secuencias Deposicionales, Facies Y Evolución Paleogeográfica," in *Basque Country UPV-EHU* (Bilbao: Univ. Basque Country).

Baceta, J. I., Pujalte, V., Serra-Kiel, J., Robador, A., and Orue-Etxebarría, X. (2004). El Maastrichtiense Final, Paleoceno E Ilerdiense Inferior De La Cordillera Pirenaica, in Geología De España Madrid. *(Soc. Geol. Esp.-Inst. Geol. Min. Esp.)*, 308–313.

Baceta, J. I., Pujalte, V., Wright, V. P., and Schmitz, B. (2011). "Carbonate Platform Models, Sea-Level Changes and Extreme Climatic Events During the Paleocene–early Eocene Greenhouse Interval: A Basin–Platform–Coastal Plain Transect Across the Southern Pyrenean Basin," in *Pre-Meeting Field-Trips Guidebook*. Eds. C. Arenas, L. Pomar and F. Colombo, 101–150. 28th IAS Meeting, Zaragoza. Soc. Geol. Esp., 7.

Basso, D. (2012). Carbonate Productivity by Calcareous Red Algae and Global Change. *Geodiversitas* 34, 13–33. doi: 10.5252/g2012n1a2

Basso, D., Coletti, G., Alice-Bracchi, V., and Yazdi-Moghadam, M. (2019). Lower Oligocene Coralline Algae of the Uromieh Section (Qom Formation, NW Iran)

and the Oldest Record of *Titanoderma Pustulatum* (Corallinophycidae, Rhodophyta). *Riv. Ital. Paleont. Strat.* 125, 197–218.

Berger, S. (2006). Photo-Atlas of Living Dasycladales. *Carn. Geol*:348pp. doi: 10.4267/2042/5831

Berger, S., and Kaever, M. J. (1992). "Dasycladales," in *An Illustrated Monograph of a Fascinating Algal Order* (Stuttgart: G. Thieme Verlag).

BouDagher-Fadel, M. K. (2018). *Evolution and Geological Significance of Larger Benthic Foraminifera. 2nd Ed* (London: UCL Press). doi: 10.14324/111.9781911576938

Bracchi, V. A., Caronni, S., Meroni, A. N., Burguett, E. G., Atzori, F., Cadoni, N., et al. (2022). Morphostructural Characterization of the Heterogeneous Rhodolith Bed at the Marine Protected Area "Capo Carbonara" (Italy) and Hydrodynamics. *Diversity* 14, 51. doi: 10.3390/d14010051

Braga, J. C. (2017). "Neogene Rhodoliths in the Mediterranean Basins," in *Rhodolith/Maërl Beds: A Global Perspective*. Eds. R. Riosmena-Rodríguez, W. Nelson and J. Aguirre (Basel, Switzerland: Springer Intern. Publ), 169–193.

Braga, J. C., and Aguirre, J. (1995). Taxonomy of Fossil Coralline Algal Species: Neogene Lithophylloideae (Rhodophyta, Corallinaceae) From Southern Spain. *Rev. Paleobot. Palynol.* 86, 265–285. doi: 10.1016/0034-6667(94)00135-7

Braga, J. C., and Aguirre, J. (2001). Coralline Algal Assemblages in Upper Neogene Reef and Temperate Carbonates in Southern Spain. *Palaeogeogr. Palaeoclimatol. Palaeoecol.* 175, 27–41. doi: 10.1016/S0031-0182(01)00384-4

Braga, J. C., and Aguirre, J. (2004). Coralline Algae Indicate Pleistocene Evolution From Deep, Open Platform to Outer Barrier Reef Environments in the Northern Great Barrier Reef Margin. *Coral Reefs* 23, 547–558. doi: 10.1007/s00338-004-0414-x

Braga, J. C., and Bassi, D. (2007). Neogene History of *Sporolithon* Heydrich (Corallinales, Rhodophyta) in the Mediterranean Region. *Palaeogeogr. Palaeoclimatol. Palaeoecol.* 243, 189–203. doi: 10.1016/j.palaeo.2006.07.014

Braga, J. C., and Martín, J. M. (1988). Neogene Coralline-Algal Growth-Forms and Their Palaeoenvironments in the Almanzora River Valley (Almeria, S.E. Spain). *Palaeogeogr. Palaeoclimatol. Palaeoecol.* 67, 285–303. doi: 10.1016/0031-0182(88)90157-5

Braga, J. C., Vescogni, A., Bosellini, F., and Aguirre, J. (2009). Coralline Algae (Corallinales, Rhodophyta) in Western and Central Mediterranean Messinian Reefs. *Palaeogeogr. Palaeoclimatol. Palaeoecol.* 275, 113–128. doi: 10.1016/j.palaeo.2009.02.022

Brandano, M. (2017). "Oligocene Rhodolith Beds in the Central Mediterranean Area," in *Rhodolith/Maërl Beds: A Global Perspective*. Eds. R. Riosmena-Rodríguez, W. Nelson and J. Aguirre (Basel, Switzerland: Springer Intern. Publ), 195–219.

Büdenbender, J., Riebesell, U., and Form, A. (2011). Calcification of the Arctic Coralline Red Algae *Lithothamnion Glaciale* in Response to Elevated CO_2. *Mar. Ecol. Progr. Ser.* 441, 79–87. doi: 10.3354/meps09405

Burke, K. D., Williams, J. W., Chandler, M. A., Haywood, A. M., Lunt, D. J., and Otto-Bliesner, B. (2018). Pliocene and Eocene Provide Best Analogues for Near-Future Climates. *Proc. Natl. Acad. Sci.* 115, 13288–13293. doi: 10.1073/pnas.1809600115

Canals, M., and Ballesteros, E. (1997). Production of Carbonate Particles by Phytobenthic Communities on the Mallorca-Menorca Shelf, Northwestern Mediterranean Sea. *Deep-Sea Res. II* 44, 611–629. doi: 10.1016/S0967-0645(96)00095-1

Canudo, J. I., Keller, G., Molina, E., and Ortiz, N. (1995). Planktic Foraminiferal Turnover and $\delta^{13}C$ Isotopes Across the Paleocene–Eocene Transition at Caravaca and Zumaya, Spain. *Palaeogeogr. Palaeoclimatol. Palaeoecol.* 114, 75–100. doi: 10.1016/0031-0182(95)00073-U

Canudo, J. I., and Molina, E. (1992). Planktic Foraminiferal Faunal Turnover and Bio-Chronostratigraphy of the Paleocene–Eocene Boundary at Zumaya, Northern Spain. *Rev. Soc Geol. Esp.* 5, 145–157.

Conti, S. (1945). "Le Corallinacee Del Calcare Miocenico (Leithakalk) Del Bacino Di Viena," *Pubbl. Ist. Geol. Univ. Genova, Genova 2(Serie a)*, 31–68.

Cornwall, C. E., Harvey, B. P., Comeau, S., Cornwall, D. L., Hall-Spencer, J. M., Peña, V., et al. (2021). Understanding Coralline Algal Responses to Ocean Acidification: Meta-Analysis and Synthesis. *Global Change Biol.* 00, 1–13. doi: 10.1111/gcb.15899

Couto, R. P., Rosas-Alquicira, E. F., Rodrigues, A. S., and Neto, A. I. (2014). The Genus *Ellisolandia* (Corallinaceae, Corallinales, Rhodophyta) in the Azores (NE Atlantic): Character Expression and Taxonomic Evaluation. *Phytotaxa* 190, 5–16. doi: 10.11646/phytotaxa.190.1.3

Denizot, M (1968). Les Algues Floridées Encoûtrantes (à l'exclusion des Corallinacées). *Mus. Nat. d'Hist. Nat., Paris, France*

Diaz-Pulido, G., Anthony, K. R. N., Kline, D. I., Dove, S., and Hoegh-Guldberg, O. (2012). Interactions Between Ocean Acidification and Warming on the Mortality and Dissolution of Coralline Algae. *J. Phycol.* 48, 32–39. doi: 10.1111/j.1529-8817.2011.01084.x

Dieni, I., Massari, F., and Poignant, A. F. (1979). Testimonianze Di Paleovene Marino in Sardegna. *Riv. Ital. Paleontol.* 85, 481–516.

Dietrich, W. O. (1927). Die Geologisch-Stratigraphischen Ergebnisse Der Routenaufnahmen durch Ostpersien-Sven Hedin, in Eine Routenaufnahmen Durch Ostpersien *Stockholm* 2, 447–464

Domingo, L., López-Martínez, N., Leng, M. J., and Grimes, S. T. (2009). The Paleocene–Eocene Thermal Maximum Record in the Organic Matter of the Claret and Tendruy Continental Sections (South-Central Pyrenees, Lleida, Spain). *Earth Planet. Sci. Lett.* 281, 226–237. doi: 10.1016/j.epsl.2009.02.025

Duller, R. A., Armitage, J. J., Manners, H. R., Grimes, S., and Dunkley Jones, T. (2019). Delayed Sedimentary Response to Abrupt Climate Change at the Paleocene-Eocene Boundary, Northern Spain. *Geology* 47, 159–162. doi: 10.1130/G45631.1

Eichenseer, H. (1988). *Facies Geology of Late Maestrichtian to Early Eocene Coastal and Shallow Marine Sediments (Tremp-Graus Basin,Northeastern Spain)* (Germany: Univ. Tübingen).

Eichenseer, H., and Luterbacher, H. (1992). The Marine Paleogene of the Tremp Region (NE Spain) - Depositional Sequences, Facies History, Biostratigraphy and Controlling Factors. *Facies* 27, 119–152. doi: 10.1007/BF02536808

Flügel, E. (1985). "Diversity and Environments of Permian and Triassic Dasycladacean Algae," in *Paleoalgology: Contemporary Research and Applications*. Eds. D. F. Toomey and M. H. Nitecki (Berlin: Springer-Verlag), 344–351.

Flügel, E. (1991). "Triassic and Jurassic Marine Calcareous Algae: A Critical Review," in *Calcareous Algae and Stromatolites*. Ed. R. Riding (Berlin: Springer-Verlag), 481–503.

Flügel, E., and Kiessling, W. (2002). "Patterns of Phanerozoic Reef Crises," in *Phanerozoic Reef Patterns*. Eds. W. Kiessling, E. Flügel and J. Golonka (USA: SEPM Sp. Publ. 72), 691–733.

Foslie, M (1909) *Algologiske Notiser VI. Kongelige Norske Videnskabers Selskabs Skrifter* 1909(2), 1–63.

Fravega, P. (1984). *Archaeolithothamnium Airoldii* Nomen Novum Ex *Lithothamnium Stefanini* Airoldi. *Riv. Ital. Paleontol. Stratigr.* 90, 103–108.

Fravega, P., Piazza, M., and Vannucci, G. (1989). *Archaeolithothamnium* Rothpletz. Indicatore Ecologico-Stratigrafico? *Atti 3° Simp. Ecol. Paleoecol. Com. Benton.*, 729–743.

Garbary, D. J., and Johansen, H. M. (1982). Scanning Electron Microscopy of *Corallina* and *Haliptilon* (Corallinaceae Rhodophyta): Surfaces Features and Their Taxonomic Implications. *J. Phycol.* 18, 211–219. doi: 10.1111/j.1529-8817.1982.tb03176.x

Gattuso, J. P., and Hansson, L. (2011). "Ocean Acidification: Background and History," in *Ocean Acidification*. Eds. J. P. Gattuso and L. Hansson (UK:Oxford University Press), 1–20.

Ghosh, A. K., and Maithy, P. K (1996). On the Present Status of Coralline Red Alga *Archaeolithothamnium* Roth. From India.. *The Palaeobot* 45, 64–70

Gibbs, S. J., Bown, P. R., Sessa, J. A., Bralower, T. J., and Wilson, P. A. (2006a). Nannoplankton Extinction and Origination Across the Paleocene-Eocene Thermal Maximum. *Science* 314, 1770–1773. doi: 10.1126/science.1133902

Gibbs, S. J., Bralower, T. J., Bown, P. R., Zachos, J. C., and Bybell, L. M. (2006b). Shelf and Open-Ocean Calcareous Phytoplankton Assemblages Across the Paleocene-Eocene Thermal Maximum: Implications for Global Productivity Gradients. *Geology* 34, 233–236. doi: 10.1130/G22381.1

Guy-Haim, T., Silverman, J., Raddatz, S., Wahl, M., Israel, A., and Rilov, G. (2016). The Carbon Turnover Response to Thermal Stress of a Dominant Coralline Alga on the Fast Warming Levant Coast. *Limnol. Ocecanogr.* 61, 1120–1133. doi: 10.1002/lno.10279

Guy-Haim, T., Silverman, J., Wahl, M., Aguirre, J., Noisette, F., and Rilov, G. (2020). Epiphytes Provide Micro-Scale Refuge From Ocean Acidification. *Mar. Exper. Res.* 161, 105093. doi: 10.1016/j.marenvres.2020.105093

Hall-Spencer, J., Rodolfo-Metalpa, R., Martin, S., Ransome, E., Fine, M., Turner, S. M., et al. (2008). Volcanic Carbon Dioxide Vents Show Ecosystem Effects of Ocean Acidification. *Nature* 454, 96–99. doi: 10.1038/nature07051

Hamon, Y., Deschamps, R., Joseph, P., Garcia, D., and Chanvry, E. (2016). New Insight of Sedimentological and Geochemical Characterization of Siliciclastic-Carbonate Deposits (*Alveolina* Limestone Formation, Graus-Tremp Basin, Spain). *Bull. Soc. Geol. Fr.* 187, 133–153. doi: 10.2113/gssgfbull.187.3.133

Hansen, J., Sato, M., Russel, G., and Kharecha, P. (2013). Climate Sensitivity, Sea Level and Atmospheric Carbon Dioxide. *Philos. Trans. R. Soc A* 371, 20120294. doi: 10.1098/rsta.2012.0294

Haynes, L. L., and Hönisch, B. (2020). The Seawater Carbon Inventory at the Paleocene-Eocene Thermal Maximum. *Proc. Nat. Am. Sc.* 117, 24088–24095. doi: 10.1073/pnas.2003197117

Hönisch, B., Ridgwell, A., Schmidt, D. N., Thomas, E., Gibbs, S. J., Sluijs, A., et al. (2012). The Geological Record of Ocean Acidification. *Science* 335, 1058–1063. doi: 10.1126/science.1208277

Hottinger, L. (1960). Recherches Sur Les Alvéolines Du Paléocène Et De l'Eocène. *Schweiz. Palaeontolo. Abh.* 75–76, 1–243.

Hottinger, L., and Schaub, H. (1960). Zur Stufeneinteilung Das Paleocaens Uns Das Eocaens. Einführung Der Stufen Ilerdien Und Biarritzien. *Eclog. Geol. Helv.* 53, 453–479.

Howe, M. A. (1919a). Tertiary Calcareous Algae From the Island of St. Bartholomew, Antigua and Anguilla. *Carn. Insti. Washington Publ.* 291, 11–20.

Howe, M. A. (1919b). On Some Recent and Fossil Lithothamnieae of the Panama Canal Zone. *U.S. Nat. Hist. Mus. Bull.* 103, 2–6.

Howe, M. A. (1934). Eocene Marine Algae (Lithothamnieae) From the Sierra Blanca Limestone. *Bull. Geol. Soc Am.* 45, 507–518. doi: 10.1130/GSAB-45-507

Jeong, S. Y., Nelson, W. A., Sutherland, J. E., Peña, V., Le Gall, L., Diaz-Pulido, G., et al. (2021). Corallinapetrales and Corallinapetraceae: A New Order and New Family of Coralline Red Algae Including *Corallinapetra* Gabriellii Comb. Nov. *J. Phycol.* doi: 10.1111/jpy.13115-20-107

Johnson, J. H. (1957). Geology of Saipan, Mariana Islands. *Calcareous algae. U.S. Geol. Sur. Prof. Paper ROM 280*, 209–246.

Johnson, J. H. (1964). Eocene Algae From Ishigaki-Shima Ryukyu-Retto. *U.S. Geol. Sur. Prof. Paper* 399, C1–C13. doi: 10.3133/pp399C

Johnson, J. H., and Stewart, W. A. (1953). Eocene Coralline Algae From Meganos Formation, California. *J. Paleontol.* 27, 130–136.

Johnson, J. H., and Tafur, I. A. (1952). Coralline Algae From the Eocene Atascadero Limestone. *J. Paleontol.* 26, 537–543.

Kamenos, N. A., Burdett, H. I., Aloisio, E., Findlay, H. S., Martin, S., Longbone, C., et al. (2013). Coralline Algal Structure Is More Sensitive T Orate, Rather Than the Magnitude, of Ocean Acidification. *Glob. Change Biol.* 19, 3621–3628. doi: 10.1111/gcb.12351

Keij, A. J. (1963). *Distichoplax* in Sarawak and North Borneo. *Bull. Br. Born. Geol. Sur.* 4, 153–160.

Keij, A. J. (1964). *Distichoplax* From Kudat Peninsula and Bangui Island, Sabah, Borneo. *Rev. Micropaléontol.* 7, 115–118.

Kelly, D. C., Bralower, T. J., and Zachos, J. C. (1998). Evolutionary Consequences of the Latest Paleocene Thermal Maximum for Tropical Planktonic Foraminifera. *Palaeogeogr. Palaeoclimatol. Palaeoecol.* 141, 139–161. doi: 10.1016/S0031-0182(98)00017-0

Kennett, J. P., and Stott, L. D. (1991). Abrupt Deep-Sea Warming, Palaeoceanographic Changes and Benthic Extinctions at the End of the Palaeocene. *Nature* 353, 225–229. doi: 10.1038/353225a0

Kiessling, W. (2010). Geologic and Biotic Controls on the Evolution of Reefs. *Ann. Rev. Ecol. Evol. Syst.* 40, 173–192. doi: 10.1146/annurev.ecolsys.110308.120251

Koch, P. L., Zachos, J. C., and Gingerich, P. D. (1992). Correlation Between Isotope Records in Marine and Continental Carbon Reservoirs Near the Paleocene/Eocene Boundary. *Nature* 358, 319–322. doi: 10.1038/358319a0

Lemoine, M. P. (1924). Contribution a L'étude Des Corallinacees Fossiles. VII. Mélobésiées Miocènes Recueillies Par M. Boucart En Albanie. *Bull. Soc. Géol. Fr.* 23, 275–283.

Lemoine, M. P. (1928). Un Nouveau Genre De Mélobésiées: *Mesophyllum. Bull. Soc. Bot. Fr.* 5, 251–254. doi: 10.1080/00378941.1928.10836268

Lemoine, M. P. (1939). Les Algues Calcaires Fossiles De l'Algérie. Matériaux Pour La Carte Géologique De L'Algérie. *1er Paléontol.* 9, 1–128.

Lemoine, M. P., and Mengaud, L. (1934). Algues Calcaires De L'Éocène De La Province De Santander (Espagne). *Bull. Soc Hist. Nat. Toulouse* 66, 171–180.

Li, J., Hu, X., Garzanti, E., and BouDagher-Fadel, M. (2020). Climate-Driven Hydrological Change and Carbonate Platform Demise Induced by the Paleocene-Eocene Thermal Maximum (Southern Pyrenees). *Palaeogeogr. Palaeoclimatol. Palaeoecol.* 567, 110250. doi: 10.1016/j.palaeo.2021.110250

Lunt, D. J., Elderfield, H., Pancost, R., Ridgwell, A., Foster, G. L., Haywood, A., et al. (2013). Warm Climates of the Past – a Lesson for the Future? *Phil. Trans. R. Soc*,A371. doi: 10.1098/rsta.2013.0146

Manners, H. R., Grimes, S. T., Sutton, P. A., Domingo, L., Leng, M. J., Twitchett, R. J., et al. (2013). Magnitude and Profile of Organic Carbon Isotope Records From the Paleocene–Eocene Thermal Maximum: Evidence From Northern Spain. *Earth Planet. Sc. Lett.* 376, 220–230. doi: 10.1016/j.epsl.2013.06.016

Martin, S., and Gattuso, J. P. (2009). Response of Mediterranean Coralline Algae to Ocean Acidification and Elevated Temperature. *Glob. Change Biol.* 15, 2089–2100. doi: 10.1111/j.1365-2486.2009.01874.x

Martin, S., and Hall-Spencer, J. M. (2017). "Effects of Ocean Warming and Acidification on Rhodolih/Maërl Beds," in *Rhodolith/Maërl Beds: A Global Perspective*. Eds. R. Riosmena-Rodríguez, W. Nelson and J. Aguirre (Basel, Switzerland: Springer Intern. Publ), 55–85.

Maslov, V.P. (1962). *Fossil Red Algae of USSR Trud. Institut. Akad. Nauk SSSR* 53, 1–222 (in Russian).

Mastrorilli, V. I. (1967). Nuovo Contributo Allo Studio Delle Corallinacee Dell'oligocene Ligure-Piemontese: I Reperti Della Tavoletta Ponzone. *Atti Ist. Geol. Univ. Genova* 5, 153–406.

Mastrorrilli, V. I. (1973). Flore Fossili a Corallinacee Di Alcune Localitá Venete Tra I Berici E L'Altopiano Di Asiago. *Atti. Soc Ital. Sci. Nat. Mus. civ. Stor. Nat. Milano* 114, 209–292.

McInerney, F. A., and Wing, S. L. (2011). The Paleocene-Eocene Thermal Maximum: A Perturbation of Carbon Cycle, Climate, and Biosphere With Implications for the Future. *Ann. Rev. Earth Planet. Sc.* 39, 489–516. doi: 10.1146/annurev-earth-040610-133431

Minnery, G. A. (1990). Crustose Coralline Algae From the Flower Garden Banks, Northwestern Gulf of Mexico: Controls on Distribution and Growth Morphology. *J. Sediment. Petrol.* 60, 992–1007. doi: 10.1306/D4267663-2B26-11D7-8648000102C1865D

Minnery, G. A., Rezak, R., and Bright, T. J. (1985). "Depth Zonation and Growth Form of Crustose Coralline Algae: Flower Garden Banks, Northwestern Gulf of Mexico," in *Paleoalgology: Contemporary Research and Applications*. Eds. D. F. Toomey and H. M. Nitecki (Berlin: Springer), 237–247.

Molina, E., Angori, E., Arenillas, I., Brinkhuis, H., Crouch, E. M., Luterbacher, H., et al. (2003). Correlation Between the Paleocene/Eocene Boundary and the Ilerdian at Campo, Spain. *Rev. Micropaleontol.* 46, 95–109. doi: 10.1016/S0035-1598(03)00012-6

Mudelsee, M., Bickert, T., Lear, C. H., and Lohmann, G. (2014). Cenozoic Climate Changes: A Review Based on Times Series Analysis of Marine Benthic $\delta^{18}O$ Records. *Rev. Geoph.* 52, 333–374. doi: 10.1002/2013RG000440

Murray, J. W. (1991). *Ecology and Palaeoecology of Benthic Foraminifera* (UK: Longman Sc. & Tech).

Murray, J. W. (2006). *Ecology and Applications of Benthic Foraminifera* (Cambridge: Cambridge Univ. Press).

Norris, R. D., Kirtland Turner, S., Hull, P. M., and Ridgwell, A. (2013). Marine Ecosystem Responses to Cenozoic Global Change. *Science* 341, 492–498. doi: 10.1126/science.1240543

O'Connell, L. G., James, N. P., Harvey, A. S., Luick, J., Bone, Y., and Shepherd, S. A. (2020). Reevaluation of the Inferred Relationship Between Living Rhodolith Morphologies, Their Movements, and Water Energy: Implications for Interpreting Paleoceanographic Conditions. *Palaios* 35, 543–556. doi: 10.2110/palo.2019.101

Orue-Etxebarria, X., Pujalte, V., Bernaola, G., Apellaniz, E., Baceta, J. I., Payros, A., et al. (2001). Did the Late Paleocene Thermal Maximum Affect the Evolution of Larger Foraminifers? Evidence From Calcareous Plankton of the Campo Section (Pyrenees, Spain). *Mar. Micropaleontol.* 41, 45–71. doi: 10.1016/S0377-8398(00)00052-9

Payros, A., Pujalte, V., Baceta, J. I., Bernaola, G., Orue-Etxebarria, X., Apellaniz, E., et al. (2000). Lithostratigraphy and Sequence Stratigraphy of the Upper Thanetian to Middle Ilerdian Strata of the Campo Section (Southern Pyrenees, Spain): Revision and New Data. *Rev. Soc Geol. Esp.* 13, 213–226.

Peña, V., Harvey, B. P., Agostini, S., Porzio, L., Milazzo, M., Horta, P., et al. (2020a). Major Loss of Coralline Algal Diversity in Response to Ocean Acidification. *Glob. Change Biol*. doi: 10.1111/gcb.15757

Peña, V., Vieira, C., Braga, J. C., Aguirre, J., Rösler, A., Baele, G., et al. (2020b). Radiation of the Coralline Red Algae (Corallinophycidae, Rhodophyta) Crown Group as Inferred From a Multilocus Time-Calibrated Phylogeny. *Mol. Phylog. Evol.* 150, 106845. doi: 10.1016/j.ympev.2020.106845

Perrin, C., Bosence, D. W. J., and Rosen, B. (1995). "Quantitative Approaches to Palaeozonation and Palaeobathymetry of Corals and Coralline Algae in Cenozoic Reefs," in *Marine Palaeoenvironmental Analysis From Fossils*. Eds. D. W. J. Bosence and P. A. Allison, 181–229. UK: Geol. Soc. Lond. Sp. Publ. 83.

Perrin, C., and Kiessling, W. (2010). "Latitudinal Trends in Cenozoic Reef Patterns and Their Relationship to Climate," in *Carbonate Systems During the Oligocene-Miocene Climatic Transition*. Eds. M. Mutti, W. E. Piller and C. Betzler (USA: IAS Sp. Publ. 42), 17–34.

Pfender, J. (1926). Sur Les Organismes du Nummulitique de La Colline de San Salvador Près Camarasa. *Bol. R. Acad. Esp. Hist. Nat.* 26, 321–330.

Pfender, J. (1939). Sur un calcaire phytogène du Lias inférieur d'Espagne et l'extension de ce faciès en quelques autres régions. *Bull. Soc. Vaudoise Sc. nat.* 60, 213–228.

Piller, W. E. (1994). *Nullipora Ramosissima* Reuss 1847—a Rediscovery. *Beitr. Paletontol.* 19, 181–189.

Pujalte, V., Baceta, J. I., Payros, A., Orue-Etxebarria, X., and Schmitz, B. (2000b). Upper Paleocene-Lower Eocene Strata of the Western Pyrenees, Spain: A Shelf-to-Basin Correlation. *GFF* 122, 129–130. doi: 10.1080/11035890001221129

Pujalte, V., Baceta, J. I., Schmitz, B., Orue-Etxebarria, X., Payros, A., Bernaola, G., et al. (2009a). Redefinition of the Ilerdian Stage (Early Eocene). *Geol. Acta* 7, 177–194. doi: 10.1344/105.000000268

Pujalte, V., Orue-Etxebarria, X., Schmitz, B., Tosquella, J., Baceta, J. I., Payros, A., et al. (2003). "Basal Ilerdian (Earliest Eocene) Turnover of Larger Foraminifera: Age Constraints Based on Calcareous Plankton and $\delta^{13}C$ Isotopic Profiles From New Southern Pyrenean Sections (Spain)," in *Causes and Consequences of Globally Warm Climates in the Early Paleogene*. Eds. S. L. Wing, P. D. Gingerich, B. Schmitz and E. Thomas, 205–221. USA: Boulder, Colorado, Geol. Soc. Am. Sp. Paper, 369.

Pujalte, V., Robles, S., Orue-Etxebarria, X., Baceta, J. I., Payros, A., and Larruzea, I. F. (2000a). Uppermost Cretaceous-Middle Eocene Strata of the Basque-Cantabrian Region and Western Pyrenees: A Sequence Stratigraphic Perspective. *Rev. Soc Geol. Esp.* 13, 191–211.

Pujalte, V., Schmitz, B., and Baceta, J. I. (2014). Sea-Level Changes Across the Paleocene-Eocene Interval in the Spanish Pyrenees, and Their Possible Relationship With North Atlantic Magmatism. *Palaeogeogr. Palaeoclimatol. Palaeoecol.* 393, 45–60. doi: 10.1016/j.palaeo.2013.10.016

Pujalte, V., Schmitz, B., Baceta, J. I., Orue-Etxebarria, X., Bernaola, G., Dinarés-Turell, J., et al. (2009b). Correlation of the Thanetian-Ilerdian Turnover of Larger Foraminifera and the Paleocene-Eocene Thermal Maximum: Confirming Evidence From the Campo Area (Pyrenees, Spain). *Geol. Acta* 7, 161–175. doi: 10.1344/105.000000276

Pujalte, V., Schmitz, B., and Payros, A. (2022). A Rapid Sedimentary Response to the Paleocene-Eocene Thermal Maximum Hydrological Change: New Data From Alluvial Units of the Tremp-Graus Basin (Spanish Pyrenees). *Palaeogeogr. Palaeoclimatol. Palaeoecol.* 589, 110818. doi: 10.1016/j.palaeo.2021.110818. 1.

Quaranta, F., Tomassetti, L., Vannucci, G., and Brandano, M. (2012). Coralline Algae as Environmental Indicators: A Case Study From the Attard Member (Chattian, Malta). *Geodiversitas* 34, 151–166. doi: 10.5252/g2012n1a9

Raffi, I., and De Bernardi, B. (2008). Response of Calcareous Nannofossils to the Paleocene–Eocene Thermal Maximum: Observations on Composition, Preservation and Calcification in Sediments From ODP Site 1263 (Walvis Ridge — SW Atlantic). *Mar. Micropaleontol.* 69, 119–138. doi: 10.1016/j.marmicro.2008.07.002

Ridgwell, A., and Schmidt, D. N. (2010). Past Constraints on the Vulnerability of Marine Calcifiers to Massive Carbon Dioxide Release. *Nat. Geosc.* 3, 196–200. doi: 10.1038/ngeo755

Robador, A. (2008). *El Paleoceno E Ilerdiense Inferior Del Pirineo Occidental: Estratigrafía Y Sedimentología* (Ph.D. Thesis University of the Basque Spain. Publ. Inst. Geol. Min. Esp., Ser. Tesis Doctorales 12).

Robador, A., Pujalte, V., Samsó, J. M., and Payros, A. (2009). Registro Geológico Del Máximo Térmico Del Paleoceno-Eoceno En El Parque Nacional De Ordesa Y Monte Perdido (Pirineo Central). *Geogaceta* 46, 111–114.

Rösler, A., Perfectti, F., Peña, V., Aguirre, J., and Braga, J.C. (2017). Timing of the Evolutionary History of Corallinaceae (Corallinales, Rhodophyta). *J. Phycol.* 53, 567–576.

Sarkar, S. (2018). The Enigmatic Palaeocene-Eocene Coralline *Distichoplax*: Approaching the Structural Complexities, Ecological Affinities and Extinction Hypotheses. *Mar. Micropaleontol.* 139, 72–83. doi: 10.1016/j.marmicro.2017.12.001

Schaub, H. (1951). Stratigraphie Und Paläontologie Des Schlierenflysches Mit Besonderer Berücksichtigung Der Paleocaenen Und Untereocaenen Nummuliten Und Assilinen. *Schw. Paläontol. Abh.* 68, 1–222.

Schaub, H. (1973). "La Sección De Campo (Prov. De Huesca: Enadimsa)," in *Libro-Guía Del XIII Coloquio Europeo De Micropaleontología*. Ed. Enadimsa, (España), 139–158.

Scheibner, C., Rasser, M. W., and Mutti, M. (2007). The Campo Section (Pyrenees, Spain) Revisited: Implications for Changing Benthic Carbonate Assemblages Across the Paleocene-Eocene Boundary. *Palaeogeogr. Palaeoclimatol. Palaeoecol.* 248, 145–168. doi: 10.1016/j.palaeo.2006.12.007

Scheibner, C., and Speijer, R. P. (2008). Late Paleocene-Early Eocene Tethyan Carbonate Platform Evolution – A Response to Long- and Short-Term Paleoclimatic Change. *Earth-Sc. Rev.* 90, 71–102. doi: 10.1016/j.earscirev.2008.07.002

Scheibner, C., Speijer, R. P., and Marzouk, A. (2005). Larger Foraminiferal Turnover During the Paleocene/Eocene Thermal Maximum and Paleoclimatic Control on the Evolution of Platform Ecosystems. *Geology* 33, 493–496. doi: 10.1130/G21237.1

Schmitz, B., and Pujalte, V. (2003). Sea-Level, Humidity, and Land-Erosion Records Across the Initial Eocene Thermal Maximum From a Continental-Marine Transect in Northern Spain. *Geology* 31, 689–692. doi: 10.1130/G19527.1

Schmitz, B., and Pujalte, V. (2007). Abrupt Increase in Seasonal Extreme Precipitation at the Paleocene–Eocene Boundary. *Geology* 35, 215–218. doi: 10.1130/G23261A.1

Segonzac, G., and Charollais, J. (1974). Sur Quelques Algues Calcaires (Corallinacées, Payssoneliacées) Des Calcaires À Petites Nummulites Des Chaînes Subalpines Septentrionales (Massif Des Bornes, Haute-Savoie, France). *Arch. Sc. Genève* 27, 111–132.

Serra-Kiel, J., Canudo, J. I., Dinarés-Turell, J., Molina, E., Ortiz, N., Pascual, J. O., et al. (1994). Cronoestratigrafía De Los Sedimentos Marinos Del Terciario Inferior De La Cuenca De Graus-Tremp (Zona Central Surpirenaica). *Rev. Soc Geol. Esp.* 7, 273–297.

Serra-Kiel, J., Hottinger, L., Caus, E., Drobne, K., Ferràndez, C., Jauhri, A. K., et al. (1998). Larger Foraminiferal Biostratigraphy of the Tethyan Paleocene and Eocene. *Bull. Soc Géol. Fr.* 169, 281–299.

Serra-Kiel, J., Vicedo, V., Baceta, J. I., Bernaola, G., and Robador, A. (2020). Paleocene Larger Foraminifera From the Pyrenean Basin With a Recalibration of the Paleocene Shallow Benthic Zones. *Geol. Acta* 18.8, 1–69. doi: 10.1344/GeologicaActa2020.18.8

Sluijs, A., Bowen, G. J., Brinkhuis, H., Lourens, L. J., and Thomas, E. (2007). "The Palaeocene–Eocene Thermal Maximum Super Greenhouse: Biotic and Geochemical Signatures, Age Models and Mechanisms of Global Change," in *Deep-Time Perspectives on Climate Change: Marrying the Signal From Computer Models and Biological Proxies*. Eds. M. Williams, A. M. Haywood, F. J. Gregory and D. N. Schmidt (London: Micropalaeontol. Soc., Geol. Soc., Sp. Publ), 323–349.

Speijer, R. P., and Morsi, A. M. M. (2002). Ostracode Turnover and Sea-Level Changes Associated With the Paleocene-Eocene Thermal Maximum. *Geology* 30, 23–26. doi: 10.1130/0091-7613(2002)030<0023:OTASLC>2.0.CO;2

Speijer, R. P., Scheibner, C., Stassen, P., and Morsi, A. M. M. (2012). Response of Marine Ecosystems to Deep-Time Global Warming: A Synthesis of Biotic Patterns Across the Paleocene-Eocene Thermal Maximum (PETM). *Aust. J. Earth Sc.* 105, 6–16.

Stockar, R. (1997). Contributo Alla Conoscenza Dell'eocene Nel Canton Ticino: L'associazione Ad Alghe Calcaree Fossili Di Prella (Mendrisiotto). *Boll. Soc Ticinese Sci. Nat.* 85, 23–46.

Stockar, R. (2000). Fossil Coralline Algae From the Paleocene Montorfano Member Type-Section (Tabiago Formation, Northern Italy). *Eclog. Geol. Helv.* 93, 409–427.

Taylor, J. D., and Glover, E. A. (2006). Lucinidae (Bivalvia) – the Most Diverse Group of Chemosymbiotic Molluscs. *Zool. J. Lin. Soc* 148, 421–438. doi: 10.1111/j.1096-3642.2006.00261.x

Thomas, E. (1990). "Late Cretaceous Through Neogene Deep-Sea Benthic Foraminifers (Maud Rise, Weddell Sea, Antarctica)," in *Proceedings of the Ocean Drilling Program, Scientific Results*, vol. 113 . Ed. P. F. Barker, J. P. Kennett, S. O'Connell, S. Berkovitz, W. R. Bryant, L. H. Burckle, et al (Texas, USA: Texas A & M University, College Station), 571–594.

Thomas, E. (2003). "Extinction and Food at the Seafloor: A High-Resolution Benthic Foraminiferal Record Across the Initial Eocene Thermal Maximum, Southern Ocean Site 690," in *Causes and Consequences of Globally Warm Climates in the Early Paleogene*, vol. 369 . Eds. S. L. Wing, P. D. Gingerich, B. Schmitz and E. Thomas, 319–332. USA: Geol. Soc. Am. Sp. Publ.

Thomas, E. (2007). "Cenozoic Mass Extinctions in the Deep Sea: What Perturbs the Largest Habitat on Earth?," in *Large Ecosystem Perturbations: Causes and Consequences*, vol. 424 . Eds. S. Monechi, R. Coccioni and M. R. Rampino, 1–23. USA: Geol. Soc. Am. Sp. Papers.

Thomas, E., and Shackleton, N. J. (1996). "The Paleocene-Eocene Benthic Foraminiferal Extinction and Stable Isotope Anomalies," in *Correlation of the Early Paleogene in Northwest Europe*, vol. 101 . Eds. R. W. O. B. Knox, R. Corfield and R. E. Dunay, 401–441. London, UK: Geol. Soc., Sp. Publ.

Vannucci, G. (1970). Microfacies a Nullipore in Un Ciottolo Calcareo Della Morena Del Garda. *Atti Istit. Geol. Univ. Gennova* 7, 427–482.

Vannucci, G., Quaranta, F., and Basso, D. (2008). Revision and Re-Documentation of M. Airoldi's Species of *Lithophyllum* From the Tertiary Piedmont Basin. *Riv. Ital. Paleontol. Stratigr.* 114, 515–528. doi: 10.13130/2039-4942/5915

Vannucci, G., Quaranta, F., and Basso, D. (2010). Revision and Re-Documentation of M. Airoldi Species of *Lithothamnion* From the Tertiary Piedmont Basin. *Riv. It. Paleont. Strat.* 116, 223–235. doi: 10.13130/2039-4942/5952

Woelkerling, W. J., Irvine, L. M., and Harvey, A. (1993). Growth-Forms in non-Geniculate Coralline Red Algae (Corallinales, Rhodophyta). *Aust. Syst. Bot.* 6, 277–293. doi: 10.1071/SB9930277

Yamaguchi, T., Norris, R. D., and Bornemann, A. (2012). Dwarfing of Ostracodes During the Paleocene–Eocene Thermal Maximum at DSDP Site 401 (Bay of Biscay, North Atlantic) and Its Implication for Changes in Organic Carbon Cycle in Deep-Sea Benthic Ecosystem. *Palaeogeogr. Palaeoclimatol. Palaeoecol.* 346-347, 130–144. doi: 10.1016/j.palaeo.2012.06.004

Zachos, J. C., Dickens, G. R., and Zeebe, R. E. (2008). An Early Cenozoic Perspective on Greenhouse Warming and Carbon-Cycle Dynamics. *Nature* 451, 279–283. doi: 10.1038/nature06588

Zachos, J. C., Röhl, U., Schellenberg, S. A., Sluijs, A., Hodell, D. A., Kelly, D. C., et al. (2005). Rapid Acidification of the Ocean During the Paleocene-Eocene Thermal Maximum. *Science* 308, 1611–1615. doi: 10.1126/science.1109004

Zeebe, R. E. (2012). History of Seawater Carbonate Chemistry, Atmospheric CO_2, and Ocean Acidification. *Ann. Rev. Earth Planet. Sc.* 40, 141–165. doi: 10.1146/annurev-earth-042711-105521

Zeebe, R. E., and Ridgwell, A. (2011). "Past Changes in Ocean Carbonate Chemistry," in *Ocean Acidification*. Eds. J. P. Gattuso and L. Hansson (UK: Oxford Univ. Press), 21–40.

Zeebe, R. E., and Westbroek, P. (2003). A Simple Model for the $CaCO_3$ Saturation State of the Ocean: The "Strangelove," the "Neritan," and the "Cretan" Ocean. *Geochem. Geoph. Geosys.* 4, 1104. doi: 10.1029/2003GC000538

Zeebe, R. E., and Zachos, J. C. (2013). Long-Term Legacy of Massive Carbon Input to the Earth System: Anthropocene Versus Eocene. *Philos. Trans. R. Soc A* 371, 20120006. doi: 10.1098/rsta.2012.0006

Conflict of Interest: The authors declare that the research was conducted in the absence of any commercial or financial relationships that could be construed as a potential conflict of interest.

Publisher's Note: All claims expressed in this article are solely those of the authors and do not necessarily represent those of their affiliated organizations, or those of the publisher, the editors and the reviewers. Any product that may be evaluated in this article, or claim that may be made by its manufacturer, is not guaranteed or endorsed by the publisher.